THE UNIVERSITY OF OKLAHOMA

GRADUATE COLLEGE

THE ELECTRICAL SHOCK TUBE PRECURSOR

A DISSERTATION

SUBMITTED TO THE GRADUATE FACULTY

in partial fulfillment of the requirements for the

degree of

DOCTOR OF PHILOSOPHY

BY

JAMES IGNATIUS MILLS, JR.

Norman, Oklahoma

1972

THE ELECTRICAL SHOCK TUBE PRECURSOR

APPROVED BY

Richard G. Fowler

Robert M. St. John

J. N. Huffaker

R. A. Day

S. B. Eliason

DISSERTATION COMMITTEE

ACKNOWLEDGEMENTS

This dissertation is not mine alone. It belongs, instead, to the many who have helped me, counseled me and kept faith in me. This fact makes it difficult to bestow proper recognition on all who deserve it and this is deeply regretted.

The author wishes to express his graditude, initially, to Professor R. G. Fowler for his help, his confidence in me, and, perhaps most importantly, for his friendship.

Drs. I. D. Latimer, R. A. Day, and M. Naraghi also deserve special recognition and thanks. Dr. Day was a great inspiration and help in the early days of the project. He taught me spectroscopy and I am grateful. Dr. Latimer was mainly responsible for the final form of the electron temperature and density diagnostics and Dr. Naraghi, of Aria Mehr University, Iran, conceived the magnetic field experiments and was responsible in part for the theoretical analysis involved.

The machine work involved was carried out with great skill by Mr. Cleve Christian, Mr. Gene Scott, and the late James Hood, Sr. Mr. Ron Stermer, an excellent glass blower, contributed his vacuum technology and many frustrating hours of his time to the cause. Special thanks are extended to Mr. Frank Maginnis of Research Instrument Company of Norman, Oklahoma, for providing the excellent ceramic spacers used in the shock tube driver. Mrs. Mary Lou Stokes typed the final manuscript. The National Science Foundation is gratefully acknowledged for supporting this work.

My co-workers in the plasma physics and fluid dynamical group at the University of Oklahoma have been a great help. Special thanks are given to Mr. R. Scott, Mr. P. Liou and Dr. R. N. Blais. The late Geoffrey Russell will never be forgotten. He initiated the investigations and made many discoveries which clarified the nature of the precursor. He also contributed segments of his personality - "It's Sydney or the Bush, Jim" - which were lessons to all of us.

This effort was not an easy one. It was frustrating at times and there were moments of doubt. Two influences allowed, indeed prompted, me to carry on. First, my wife, Susan. She strove to be patient and supported me in many other ways. Secondly, an ideal best expressed by the following:

> "What is education? I should suppose that education was the curriculum one had to run through in order to catch up with onself, and he who will not pass through this curriculum is helped very little by the fact that he was born in the most enlightened age."

Fear and Trembling
Søren Kierkegaard

DEDICATION

This dissertation is dedicated to my Mother and Father.

TABLE OF CONTENTS

TABLE OF CONTENTS (Cont'd.)

LIST OF ILLUSTRATIONS

LIST OF ILLUSTRATIONS (Cont'd.)

ABSTRACT

Observations of luminosity and ionization far in advance of the plasma-acoustic expansion in electrically driven shock tubes have been made by many investigators and the conflicting results and explanations of these studies have led to much confusion. The results described in this dissertation clarify the situation. Precursor waves were created and studied in helium by means of an electrically driven shock tube employing two different discharge circuit configurations. The component causes of precursive effects have been separated and identified and individually studied in detail. Parameters of basic interest such as wave speed and electron temperatures and densities have been monitored using nuclear data handling techniques and photomultipliers for the wave speeds and a revised spectral line ratio technique for the temperatures and densities. Velocities of the order of 10^8 to 10^9 cm/sec have been recorded. Electron temperatures of 10 eV and electron densities ranging from 10^9 to 10^{10} electrons/cm^3 have been observed. Extensive studies employing the use of a magnetic field have been conducted in order to gain insight into the thermal conduction processes acting to transfer energy to the wave front. Many investigations of the electrical properties of the wave including the use of external calibrated probes to measure the electric field strengths associated with the front have been undertaken.

A discussion of the bearing this new knowledge has on explaining past studies as well as planning future studies with the electrical shock tube is included.

THE ELECTRICAL SHOCK TUBE PRECURSOR

CHAPTER I

INTRODUCTION

Interest in fast moving luminous pulses began when the first eyes looked upward and beheld a lightning stroke crashing through the heavens. This interest became a scientific topic, rather than a mystical one, in 1705 when Francis Hauksbee [1] noted light flashes originating from an evacuated tube over a disturbed mercury column. Any speculation into the nature of such laboratory created phenomena was absent until Wheatstone [2], in 1837, postulated that these luminous pulses were actually propagating, with finite speed, from one point to another.

The years from 1837 to the beginning of the twentieth century saw the results of two more important investigations into the phenomenon. W. Von Zahn [3], in 1874, looked for a Doppler shift in the radiation from the luminous front. His failure to see such a shift offered the first proof that there exists no motion of the excited atoms. This lack of mass motion has led most investigators to argue that the waves are not basically fluid dynamical in nature. In 1893 J. J. Thomson [4] reported a front of luminosity propagating with a speed of the order of one-half light speed in a fifteen-meter long discharge tube.

Little work was done again on these waves, now referred to as ionizing potential waves or breakdown waves, until 1930, when Beams [5] confirmed Thomson's observations and offered a qualitative theory of these fronts. Beams proposed that electrons, due to their large mobilities, are primarily responsible for the propagation of these luminous fronts. The high field in the neighborhood of the pulsed electrode make possible the electrical breakdown and intense ionization of the gas in this region. Due to the large difference in the mobilities of the ions and the electrons, a space charge will be established. This space charge will result in a distortion of the potential distribution of the conducting gas in such a way as to displace the wave front away from the high voltage electrode. This process continues resulting in the continuous propagation of the luminous front. This theory has remained basically correct and serves us still. In the years following, Beams and his associates continued their investigations of the phenomenon. These investigations resulted in the gathering of a large quantity of information about the propagation speed of the event under various operations conditions [6,7,8,9]. All in all, however, little progress was made during these years in understanding the wave. The major interest appeared to be only in the initiation of fast luminous fronts from regions of high potential and their subsequent observation. Studies of the importance of the discharge tube geometries involved were never conducted. Also, there were no attempts to describe or classify the waves according to standardized tube geometries or any other set of standardized parameters.

The discovery of optically narrow luminous frontsmmoving ahead of and much faster than the plasma acoustical shock in shock tubes revived interest in the origin and nature of fast moving luminous fronts.

Hollyer [10] did the first systematic study of waves having much higher Mach numbers than predicted by theory as observed in conventional shock tubes.

In electrical shock tubes, ionizing fronts were found to move with velocities much larger than calculated for an ion acoustic shock wave mode. Perhaps more importantly, it was found that the Rankine-Hugoniot relations could not be applied to the shock front without assuming preionization of some sort.

Hales and Josephson [11] were the first to publish studies of these precursor waves in electrically driven shock tubes. Their wave propagated with a velocity on the order of 10^8 cm/sec, exhibited a negative charge, and began to propagate shortly after driver conduction was established.

The phenomenon was becoming evident to many investigators and several interesting proposals to explain the origin and nature of the precursor were formulated. Weymann [12] made detailed investigations of a luminous negative region which he detected well in front of his shock front. Weymann proposed that he was observing the diffusion of highly mobile electrons. It was never clear whether Weymann's front had a sufficiently rapid rise in electron density to warrant the label <u>wave</u> or <u>front</u>.

McLean, Kolb and Griem [13] were disturbed by the discrepancies between observation and Rankine-Hugoniot predictions in their electromagnetic T-tube. They did indeed observe some precursive luminosity. They showed that the radiation was not Rayleigh-scattered driver plasma light, as had been postulated, and suggested that they were observing, instead, photon-preionization due to a stream of ultra violet radiation originating in the driver. The difficulties with this suggestion were immediately obvious however. Propagation in an atomic gas cannot be explained by this theory. In addition, the relatively constant time history displayed by the wave could not be explained in terms of simple photoionization by u-v photons originating in the driver. One would expect such a phenomenon to exhibit an inverse square dependence.

Fowler and Hood [14] reported these waves in 1962 and in conjunction with this investigation Paxton [15] applied fluid dynamical methods to the precursor. Paxton treated the phenomenon as an electron shock wave which explained the high velocities as well as some other characteristics of the wave. More recently, Shelton [16] has carried out a detailed one-dimensional analysis of breakdown waves in general with the idea that precursors are one member of a family of such fluid-dynamical events.

Lubin and Resler [17] observed and studied in detail the precursor in an electromagnetic shock tube. They observed that the precursor velocity was linearly proportional to E/P in the driver. They observed their precursor in both hydrogen and argon. In a related study, Lubin [18] proposed the idea that precursors are the result of an electromagnetic wave propagating down a transmission line formed by the shock tube. The authority of Lubin's thesis was lessened somewhat, however, by an ad-hoc equation for the ionization process. This equation appears to have no physical justification. It should be noted that Snoddy, Beams and Dietrich [19] suggested in 1936 that the behavior of a long discharge tube was reminiscent in many ways of a transmission line.

In 1964 Haberstitch [20] postulated, without proof, that ionizing potential waves, or breakdown waves, similar to the kind of phenomenon observed and explained by Beams were solely responsible for the precursive effect observed in the electrical shock tube. He constructed a very fine apparatus to study these waves and produced a great deal of information about their nature. His work is really not applicable to the electrical shock tube, however, since he had no driver as such in his apparatus. He therefore lacked the region of intense thermal properties that is found in the electrical shock tube.

The final historical consideration will be the work of Russell [21]. Russell was successful, in 1968, in separating, via a side arm, what he considered to be a fluid-dynamical electron wave from the bright main tube luminosity which he concluded to be predominately photon produced. His studies showed the importance of the use of side arms in the study of one component of precursive effects.

It is now felt that the excessive light scattering Russell noted in the main tube was due to his high impurity concentrations.

This brief historical synopsis will probably serve to impress upon the reader that past precursor research has been characterized by some confusion. Most researchers, upon observing and studying precursive effects, have reported data agreeing as far as the more fundamental parameters are concerned. There have been, however, a wealth of different models proposed, all of which have had only limited success in explaining all properties of these waves.

The purpose of the work herein reported to resolve all components of precursive effects as observed in a particular electrical shock tube and to study in detail the properties of these components.

CHAPTER II

APPARATUS

The Shock Tube

The complete understanding of the component causes of the precursive effects observed during this investigation required several minor modifications of the shock tube. Fortunately, the basic apparatus is quite versatile and modifications on either the driving components or the expansion chamber could be done quickly and easily. The description given below will be of the basic device concentrating on constant parameters. Any changes made on the apparatus will be discussed in the chapter pertaining to experimental procedures and results.

The shock tube can be broken down into three main systems and it is convenient to do so for purposes of description. The three systems considered are the driving system, the expansion system, and the vacuum system. The driving system was composed of a power supply, energy storage capacitor, ignitron switch, driver segment, and a shielding chamber surrounding the entire affair. The expansion system consisted of one meter sections of Pyrex tube coupled together to the desired configuration, an electrostatic cage to provide a known ground array, a wooden support form, and a rail and cart system to supply mobility and support to the disgnostics. Finally, the vacuum system consisted of a mechanical forepump and an electric oil diffusion pump, cold trap for purity, a leak system for allowing the gas to enter the tube, and a McLeod gauge for monitoring the pressure. Figure 1 presents a block diagram of the shock tube.

These systems will now be considered one at a time and dealt with in detail.

The Driving System

The power supply used to charge the driving capacitor was a Plastic Capacitor 20KV, 5 ma, Power Pak. This unit was small enough to allow the mobility necessary during polarity changes and was also quite free of corona. This power supply unit contains a step up transformer, two silicon rectifiers, and two high voltage capacitors forming a voltage doubler circuit. The ripple factor on the output voltage is 1% rms or 2.7% peak to peak. The dimensions of the unit are 8"×3.75"×4.5" and the weight is 12.5 lbs. The 60 cycle AC line voltage entered the power supply through a Sola isolation transformer and an Ajust-A-Volt variable auto transformer. The output of the power supply was adjustable from 0-20KV D.C.

The output voltage of the power supply was applied through a charging resistor to the driving capacitor where the stored energy could be coupled into the gas of the discharge tube. The capacitor used was a single Sangamo 74C503 capacitor with a measured capacitance of 14.1 μF and a 0.040 μH equivalent series inductance. The capacitor could be operated at voltages up to 20KV. The capacitor is capable of supplying 40×10^3 joules/sec during discharge. Switching was accomplished by using a low inductance, low resistance G.E. 7703 ignitron.

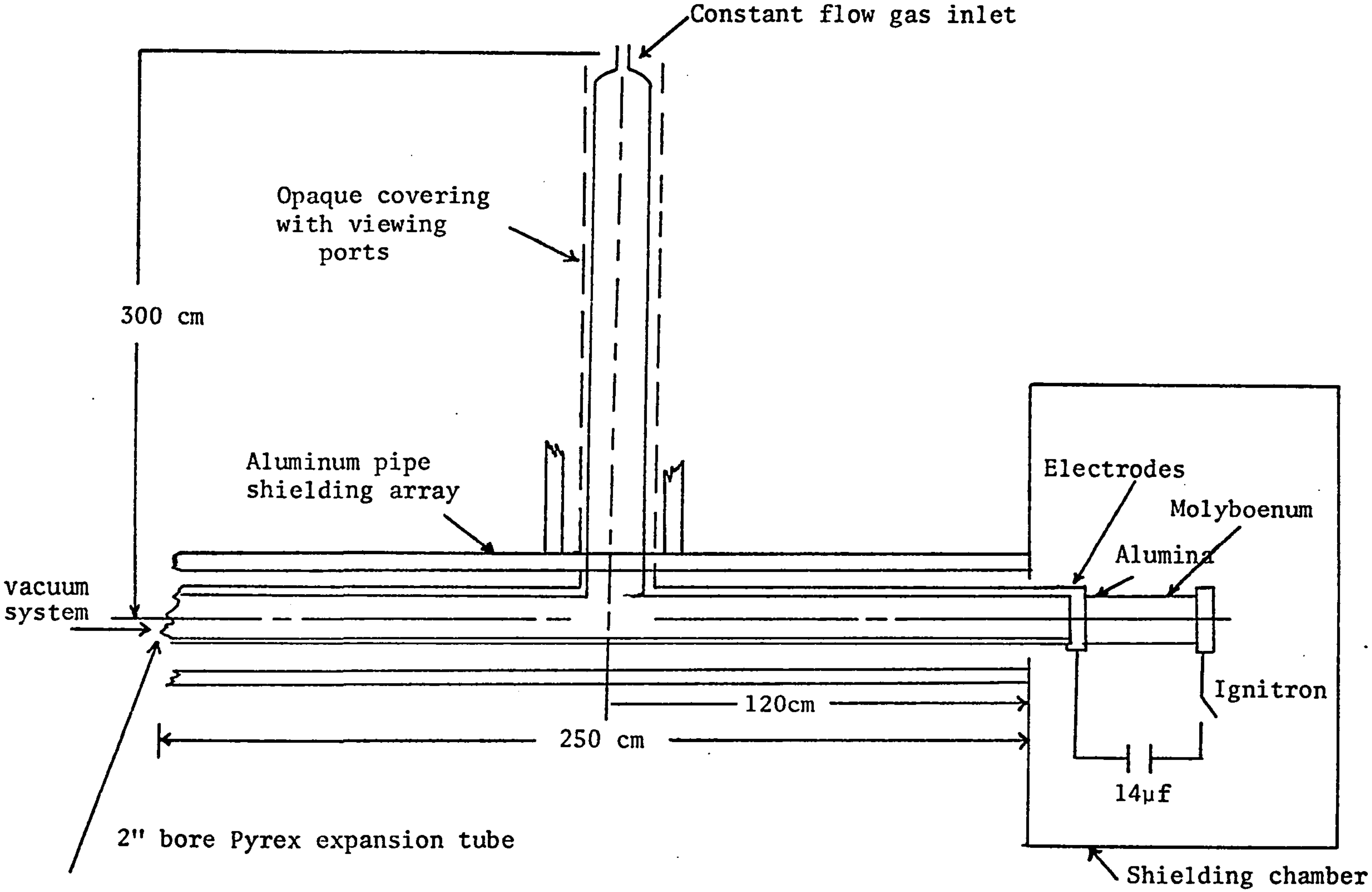

Schematic arrangement 2" diameter Oklahoma Shock Tube viewed from above.

Figure 1. The electrical shock tube.

The device is small, has adequate voltage standoff characteristics, and offers low inductance (0.03 μh) and low resistance (μ0.01 ohms) thereby producing an adequate current maximum. The breakdown delay is small enough not to present a problem.

The ignitron was fired by a separate control unit which supplied a 600V pulse via a 0.1 μf capacitor.

The energy of the capacitor was coupled to the gas via two molybdenum electrodes separated by an alumina ceramic spacer. The spacer was constructed with flared ends allowing the electrodes and the spacer to bolt together using Corning pipe flange fittings. The entire length of this driver was 10 cm. Figure 2 shows the driver construction in detail.

The two driver electrodes were coupled directly to the terminals of the discharge capacitor and one terminal was then connected to ground.

The entire system of driver, power supply components, capacitor and switching devices was confined within a metal shielding chamber which protected the diagnostic equipment from electromagnetic radiation emitted by the discharge and also reduced external interference which might affect the discharge. A shielding factor of 10^5 was measured. The driver circuit is shown in detail in Fig. 3.

The Expansion System

The expansion tube proper was constructed of Pyrex "Double Tough" pipe. Each section of the pipe was one meter long and flanged at the ends so that sections could be clamped together with aluminum

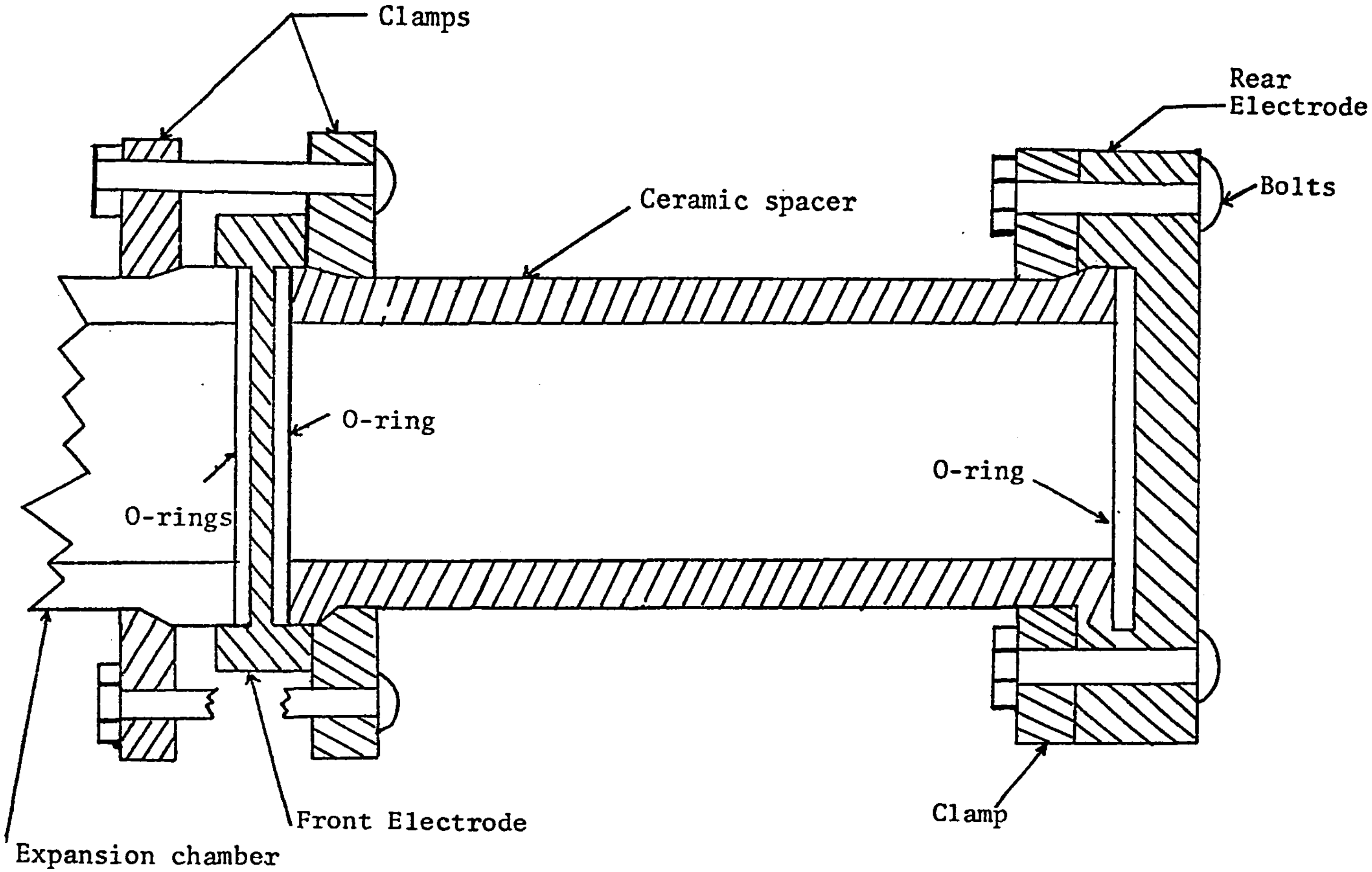

Figure 2. Detail of driver construction.

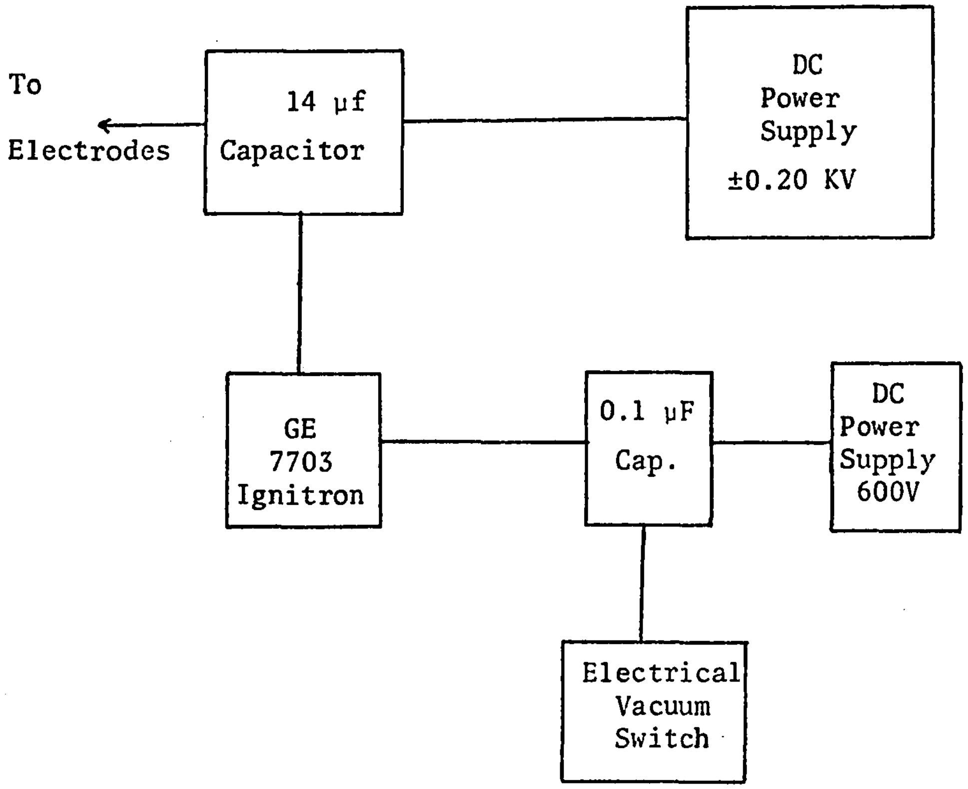

Block diagram of discharge circuit.

Figure 3. The Discharge Circuit.

clamps. The ends of the pipes were constructed with o-ring grooves and Teflon o-rings were used for the vacuum seal. The pipe could also be mated to the driver segment via o-rings and flange clamps.

The final configuration of the expansion tube consisted of a rather short main tube with a long perpendicular side arm. The work of Russell [21] was successful in showing that the major component of the shock tube precursor could best be studied in such a side arm. The main expansion tube, which was collinear to the driver segment, was 220 cm in length and had a 5 cm I.D. The side arm was three meters in length and joined the main expansion tube 110 cm from the driver.

Surrounding the expansion tube--both main tube and side arm--was an array of $1\frac{1}{4}$" aluminum pipes. These four pipes were symmetrically spaced around the main tube and the side arm and connected to the system ground. The array constituted an electrostatic ground which provided field symmetry. The presence or absence of this array proved to have no observable effect on the experimental results, however.

The entire system of expansion tube and ground array was supported by a wooden frame. In addition to functioning as support, the wooden frame insured that there was no electrical connection to ground in contact with the shock tube.

The Vacuum System

The pumping station proper consisted of a mechanical forepump and an oil diffusion pump. The mechanical forepump was a Cenco-Megavac pump which was capable of producing a vacuum of .001 torr. The pump and motor were removed from their base and remounted on a wooden board. The purpose here was to insure that no direct electrical connections to ground were made. Anticipating the possibility of this system behaving as a Van de Graaff machine, a large resistance was placed between pump and motor. The diffusion pump was a Consolidated Vacuum two-inch water cooled oil diffusion pump. The water connections to the diffusion pump were made through four meter long sections of ¼" rubber tubing. A four-meter long rubber tube full of water provides a high resistance and once again insures that no electrical connection is made to ground.

A double range McLeod gauge was calibrated and installed so that absolute pressure readings could be made. A liquid nitrogen cold trap was installed between the McLeod gauge and the rest of the vacuum system. The two pumps, cold traps and the careful maintenance of two o-ring seals allowed a base pressure of 10^{-5} torr to be achieved without difficulty.

The leak system, which allowed the gas to be studied to enter the tube, consisted of an adjustable screw valve and a gas bottle equipped with a Matheson gas pressure regulator.

The gas bottle was supported six inches above the floor by a wooden stand, again to insure that the shock tube was isolated from ground. The gas used was Matheson ultra high purity helium. The gas contained less than 7.6 p.p.m.

This careful detail to gas purity was taken only after empirical evidence pointed out how greatly impurities affected the structure of the wave. No detailed studies have been done concerning these effects but it appears likely that while the basic propagation mechanism is little affected by impurities, radiative processes such as photo-ionization of impurities can be involved.

The Penning effect, where impurities are ionized by metastable helium atoms, is no doubt a most important consideration when dealing with impurities.

Diagnostics

Photomultiplier Units

Photomultiplier units were used to observe the luminosity associated with the precursor. These observations were needed for velocity measurements, temperature and density studies, and many quantitative observations.

Three different kinds of photomultiplier (hereafter referred to as PM's) were used. The three PM's were used in various modes and according to their particular parameters of rise time, multiplication factor, etc.

RCA 931-A photomultiplier tubes were found to perform quite satisfactorily for limited applications. Their small size and fast rise time, as well as relatively inexpensive cost, make them indispensable when light intensities are fairly bright.

The glass envelope of these tubes, with the exception of the photo-cathode window, was enveloped in aluminum foil which was shorted to the anode via the base pin. The resulting decrease of anode-last stage capacitance results in a reduction of the tubes' rise time. This method is discussed by Liou [22]. The tubes have a rise time of 1 nsec.

Although fast responses are desirable and indeed necessary, they do one little good if the tubes are behaving in a non-linear fashion.

Photomultiplier saturation for the 931-A and its associated circuitry became a problem for output signals greater than 0.5V. Care was taken so that this condition would never be present. The circuit of the 931-A tubes is shown in Fig. 4.

For more sophisticated applications requiring better sensitivity without appreciably sacrificing response time two other units were used. One of these units was an RCA 7746 photomultiplier whose circuit is shown in Fig. 5. The 7746 is a ten-stage, head on, spherical faceplate tube with S-11 response. The wavelengths of maximum response. The wavelengths of maximum response for S-11 is 4400 ± 500 angstroms. This range is particularly favorable for temperature studies. The tube features an enclosed inline dynode structure. The current amplification at 1000V is 1.7 10 while the maximum cathode to anode voltage is 2500 V. The tube was normally operated at less than 2000 V. The anode-pulse rise time for the 7746 is two nanoseconds which is, although slower than the 931-A, very fast when one considers that the tube possesses ten stages and that its sensitivity is two orders of magnitude greater than that of the 931-A.

The third PM tube used was an EMI type 9558. This tube is a two-inch diameter flat-faced, end window tube with a 44 mm cathode and eleven venetian-blind dynodes of the CsSb type. The cathode is of the S-20 type which provides maximum efficiency between 3500 and 5000 Å. The gain of this tube is comparable to the RCA 7746 but the 9558 has a slower response time. For this reason the tube was used in situations requiring high gain but where a very fast rise time was not a critical factor.

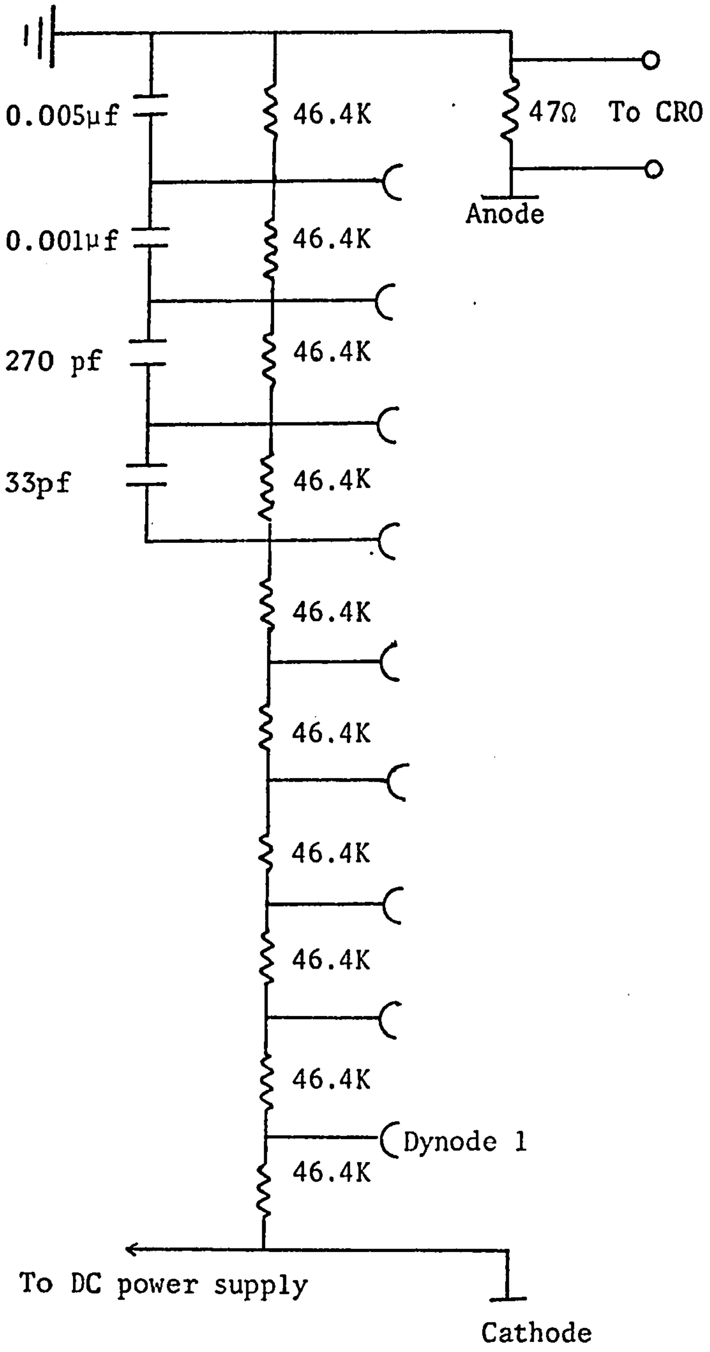

Figure 4. The 931-A Photomultiplier.

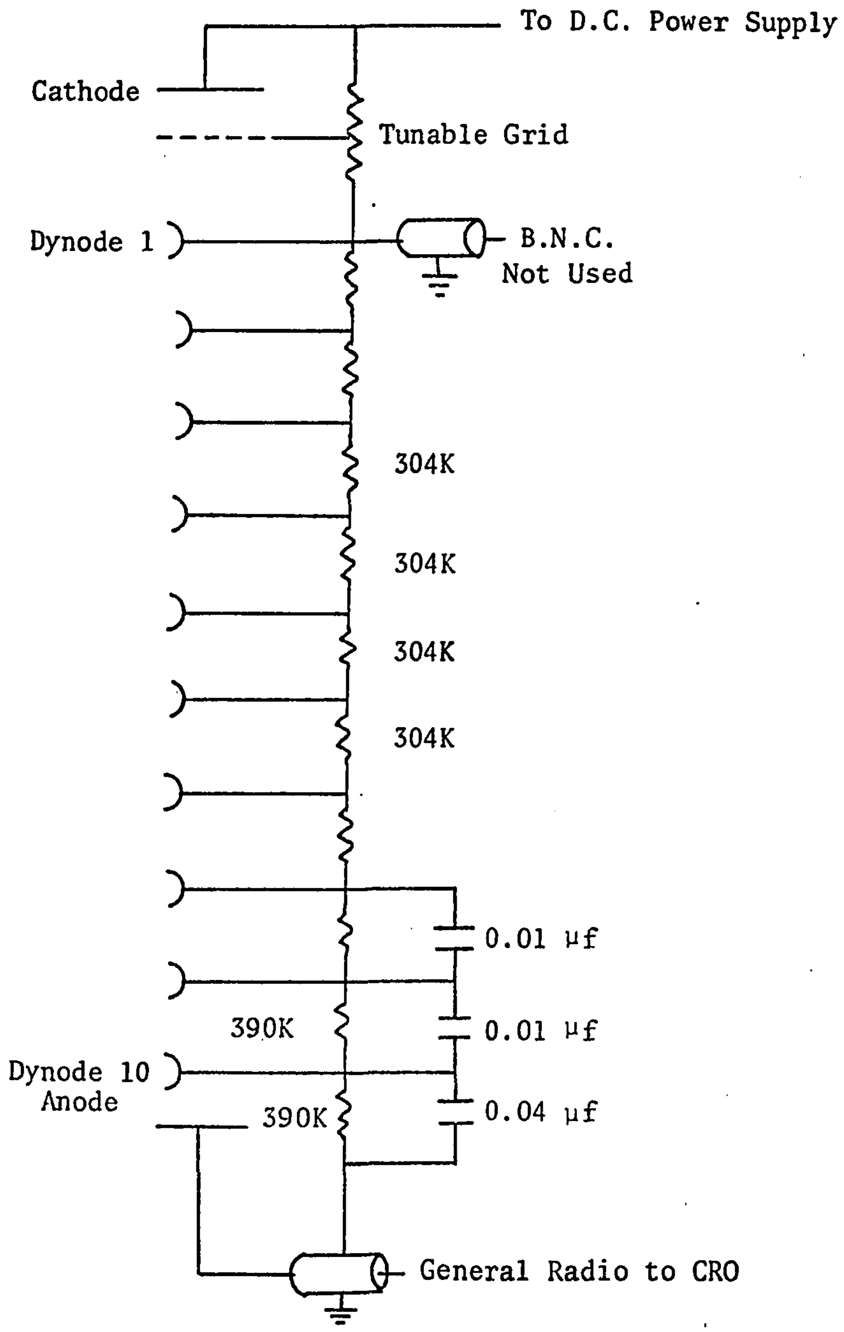

Figure 5. The 7746 Photomultiplier.

The housing for the 931-A tube was supported by ring stands. The 7746 and 9558 PM's were placed in cases which were mounted on a cart and rail assembly running parallel to the expansion chamber. The carts could easily be moved from position to position and locking screws enabled them to be secured at any desired position. A 2 mm vertical slit was installed at the end of each can.

All PM's were operated by one of the two Fluke low-ripple power supplies. A Fluke model 405 power supply with a range of -.6 to -3 KV D.C. and a Fluke model 408B with a range of 0 to -6 KV D.C. were used.

The PM signals were fed through terminated 50 ohm cables to one of three different oscilloscopes.

A Tektronix type 555 dual-beam oscilloscope was used when an oscilloscope of slow response could be tolerated. The type 555, with its dual beam capability, was particularly useful for velocity measurements. The type-L preamplifier plug-in unit used has a measured rise time of six nanoseconds. Therefore the rise time of the entire PM tube oscilloscope system was dominated by the oscilloscope regardless of the photomultiplier type used.

For measurements such as temperature and density, where one must have a very accurate record of the optical history of the front at all times, faster oscilloscopes were found necessary. A Tektronix type 519 oscilloscope was used to create a standard. This instrument has a measured rise time of 0.28 nanoseconds therefore limiting the response time of the system only to PM tubes employed. The difficulties encountered when using the 519 arise due to the low vertical sensitivity of 9.4 volts/cm. This makes low intensity measurements difficult without resorting to amplifier units which themselves contribute an additional response time consideration.

The third type of oscilloscope used was the very convenient Tektronix type 545 oscilloscope. The rise time of this oscilloscope at 2.3 nanoseconds is slower than the 519 but considerably faster than the 555. The mechanical size of the instrument, allowing great mobility, and its sensitivity made it very useful for most applications. Traces taken with the 454 were compared to those taken on the 519 to insure that the 454 was giving an accurate time history of the event. In every situation it was found that the response of the 454 was sufficient to satisfy even the most demanding experimental considerations.

Temperature and Density Diagnostics

The method used to obtain the electron temperatures and densities associated with the precursor required the observation of the time history of individual spectral lines in the luminous front. To obtain this information, two diagnostic systems were constructed and used.

Initial studies were made using a Hilger E612 spectrograph in conjunction with 931-A photomultipliers. The photographic plate holder was modified so that two photomultipliers could be set to observe two different helium spectral lines simultaneously. The alignment of the PM's was achieved using a helium Geisler tube. The individual lines of interest were brought through a system of slits and lenses to focus on the photo-cathode of the PM tube. The disadvantages of this system were two-fold. There is the obvious difficulty in alignment and then, too, the mechanical size of the Hilger makes measurements at different tube locations a most impressive task.

After empirical data indicated that simultaneous records of the two spectral lines resulted in the same conclusions obtained by separate observations, a simpler more versatile device was utilized for these measurements. A Jarrell-Ash quarter meter monochromator with adjustable entrance and exit slits was used. Typical applications required the use of 0.20 mm entrance slit and a 0.28 mm exit slit. Mounted coaxially with the exit slit was the RCA 7746 PM tube previously described.

The advantages of this system were many. The monochromator was calibrated using a He-Ne laser and a helium Geisler tube. Very accurate spectral line alignments are possible. In addition to this advantage, the monochromator also allowed investigations at lower intensities due to the use of the more sensitive PM. The monochromator-PM system was mounted on the cart-rail apparatus thus allowing quick and easy alignment at varying distances along the expansion tube.

All temperature and density measurements reported in this work were made using the monochromator-PM system. Initial studies of wave temperatures and densities relying on the Hilger spectrograph and 931-A PM tubes have been reported in an earlier work. [23]

Magnetic Field Experiments

Magnetic field experiments were made using a General Electric water cooled electromagnet with nine centimeter diameter cylindrical pole pieces. A maximum transverse magnetic field of 2000 Gauss was possible for continuous duty. For short intervals, however, the field could be increased to 2600 Gauss. The gap between pole pieces was adjusted to 10 cm in order to provide sufficient room for the side arm of the shock tube. Fringing effects were measured and found to be very small.

A separate electromagnet in the form of a solenoid was used for studies of the effects of an axial magnetic field upon the wave. Fields up to 1000 Gauss with continuous operation were available. The inside diameter of the solenoid was 10 cm more than required in order for the side arm to be positioned inside the magnet.

Both magnets were energized by a low ripple D.C. generator. The current through the magnet was either controlled at the generator or by means of a series rheostat. A precision D.C. ammeter was used to measure the circuit current.

For measurements relative to the magnetic induction experiments, two pieces of No. 14 copper wire were inserted a distance of one millimeter into a meter section of Pyrex "Double Tough" pipe. This section could be fitted into the expansion chamber of the shock tube at any time. A bridge circuit was used to detect any voltage across the electrodes. At times a nine volt D.C. battery was used to bias the electrodes.

Axial Electric Field Probes

For measurement of the axial electric fields associated with the front, a differential probe was employed. The construction of these probes is shown in Fig. 6. Coaxial construction was used to eliminate loops in the probe circuit which might give spurious inductive signals. The connecting cable was a 50 ohm coaxial cable, with the outer insulation removed, that was placed inside four millimeter Pyrex tubing. The inner conductor was soldered to a tapered conical tip, and

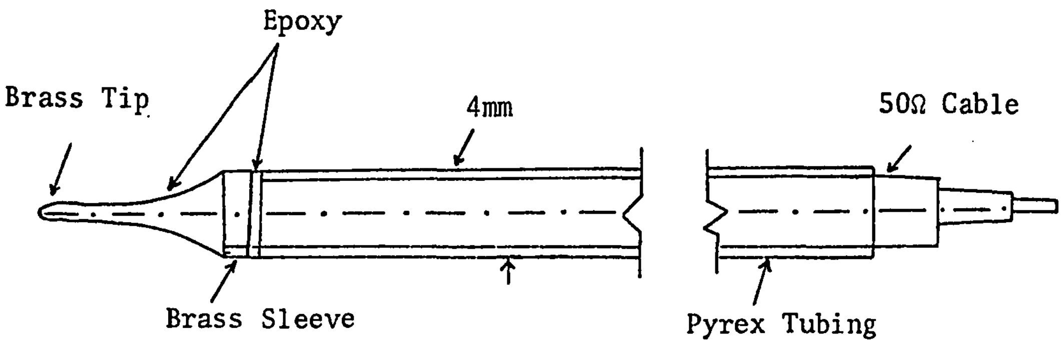

Construction of the electric probe.

Figure 6. The axial electric field probe.

the outer conductor to a sleeve. Both the tip and sleeve were constructed from brass. The inner and outer conductor pieces were separated by a distance of one centimeter. The space between the two conducting pieces, or the electrodes, was filled with a low vapor pressure epoxy.

These probes were used in two modes. One variation was to emerse the probe inside the plasma to measure the electric field due to the charge separation at the front. The reliability of such techniques is, of course, questionable due to the disturbing effect the probe will have on the plasma flow around it.

When the probes were used in this mode, a vacuum "quick coupling" was used to enter the probe into the shock tube.

A calibrated version of these probes were used to measure the field strength of the quasi-D.C. electromagnetic fields driving one component of the wave. These probes, which were essentially dipole antennas, were calibrated at 1.5 MH using a radio receiver in conjunction with a standard signal generator and the signals transmitted by a local radio station. A signal of one volt on an oscilloscope corresponded to 500 volts/cm in the plasma.

Other minor pieces of diagnostic equipment were used for specialized applications and will be described in the appropriate sections of experimental procedures and results.

CHAPTER III

EXPERIMENTAL PROCEDURE AND RESULTS

Identification of Precursor Components

Before a systematic experimental procedure could be formulated, it was necessary to investigate the precursive effects in a qualitative manner in order to identify the mechanisms which created and propagated the luminous fronts called precursors.

It has been mentioned that Russell had, through the use of a side arm off the main tube, succeeded in isolating from the intense luminosity in the main expansion chamber of the shock tube what appeared to be a fluid wave with a definite front and traveling at 10^8 cm/sec. Russell was unable to show whether or not this wave was also present in the main expansion chamber of the shock tube. At the time, in fact, it appeared that photon produced light was the major component of the luminosity observed in the main tube and it was thought possible that the relatively low-intensity luminous front observed in the side arm might be created by some process initiated when the photon produced phenomenon passed the junction of main tube and side arm.

This work began with an attempt to establish if indeed there did exist a wave in the main tube and if so, to determine what, if any dependence upon photoionization the wave had.

To accomplish this goal a second side arm was introduced one meter downstream from the first. Matched pairs of RCA 931-A PM's were set twenty centimeters down each side arm. A time delay between the arrival of the fronts in the two side arms was observed and this time delay corresponded exactly to flights from a common point. Liou found that the positioning of a PM near the head of the first side arm as a reference point allowed one to track this wave along the main expansion chamber even in the presence of the photon produced luminosity. Figure 7 demonstrates the time delay observed at identical vantage points in the two side arms.

It has been suggested by some observers that photoionization of impurities could well be the source of precursive effects in electrical shock tubes. Appleton [24] suggested that photoionization of an impurity, such as oxygen, of only one part per million in argon gas could explain the electron and ion densities observed in the region ahead of moderately strong shocks in argon. With considerations such as this in mind, the 99.95 per cent He employed by Russell was replaced by the ultra pure He described previously and the vacuum system was redesigned to insure a much cleaner environment. When this was accomplished there was a striking reduction of the scattered luminosity observed in the main expansion tube. In fact, the profile of the wave phenomenon was now clearly present and the wave could be tracked continuously from about .5 meters in front of the driver to a point in the side arm where the wave abruptly ceased to exist.

Some photon induced luminosity was still present to be sure, but this effect is minor compared to the fluid wave and the luminosity drops off rapidly, as $1/r^2$.

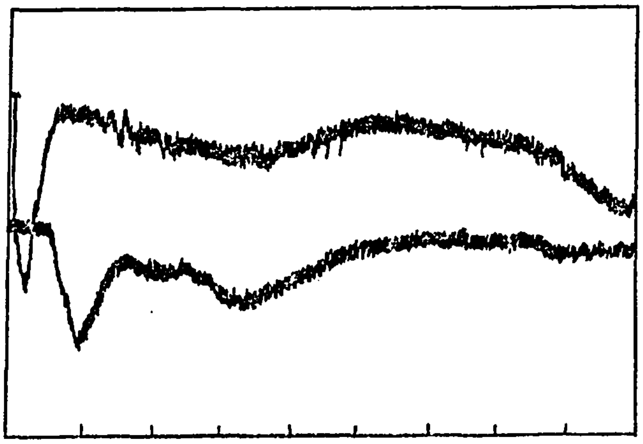

P = .750 Torr in Helium

500 nsec/cm

Oscillogram illustrating time delay between the arrival of wave at two different sidearms separated by 113 cm.

Figure 7. The time delay observed in two side arms separated by 113 centimeters.

The fluid wave, hereafter called simply the precursor, is not affected by the photoionization as indicated by the continuous advance of the precursor front down the main tube and into the side arm where driver originating photons cannot reach.

Having thus established that the wave precursor was a unique phenomenon associated in some way with the driver discharge, more qualitative experiments were conducted to clarify the nature of the wave.

Russell had looked for any influence of electrical geometry on the wave precursor by introducing various configurations of cans around the side arm, and connecting these cans to the electrodes of the driver, and had found no effect. These experiments were continued in an attempt to shed further light on the electrical properties of the wave and at the same time to eliminate arguments that stray electric fields might create precursive results under the proper conditions.

The first experiment consisted of inserting a one-half meter long, two-inch I.D. section of brass pipe between the side arm and main tube. The ends of the pipe were fitted with collars machined with o-ring grooves so that the pipe could be mated coaxially with the Pyrex "Double Tough" pipe. This arrangement presented no fluid-dynamical discontinuities.

The wave would reappear at the far end of the pipe having apparently propagated through with the proper transmission speed. It was possible to place a 65 per cent transmitting wire screen across the entrance to the tube and still observe apparent propagation of the wave with only a modest reduction in the intensity of the reappearing wave. The metal cylinder and grid combination was now connected to the room ground and experiments were conducted once again. This grounding resulted in a dramatic suppression of the wave. Two 931-A tubes were stationed fifty-seven centimeters apart on the far end of the brass pipe to form a speedometer. Comparisons of the wave structure before and after grounding the pipe are shown in Fig. 8.

The observed suppression of the wave upon encountering the grounded metal pipe and grid clearly indicated that the energy of the precursor might well be derived from an electric field associated with the driver and would thus be identifiable as a breakdown wave. The idea that the wave might be a breakdown wave was further supported by an experimental result which we had long observed. If one uses a loop probe to monitor the current in the driver and compares this record with the onset of the wave, it is easily established that the wave is always initiated in the general vicinity of the inflection point on the current rise. This apparent dependence on dI/dt was a clear indication of a possible reliance of the wave on the generation of an electric field in the driver.

In order for a breakdown wave to be present in an apparatus it is necessary to have a region of high potential with respect to infinity. A study of the discharge circuit of the shock tube was therefore undertaken to establish whether or not there existed an improper grounding which would allow one electrode to rise in potential with respect to ground thus becoming the driving electrode for a breakdown wave. If the grounded electrode of an electrical shock tube is truly at ground, then it would appear that the only breakdown wave possible would be one

Cylinder
Floating
500 nsec/cm
1 v/cm

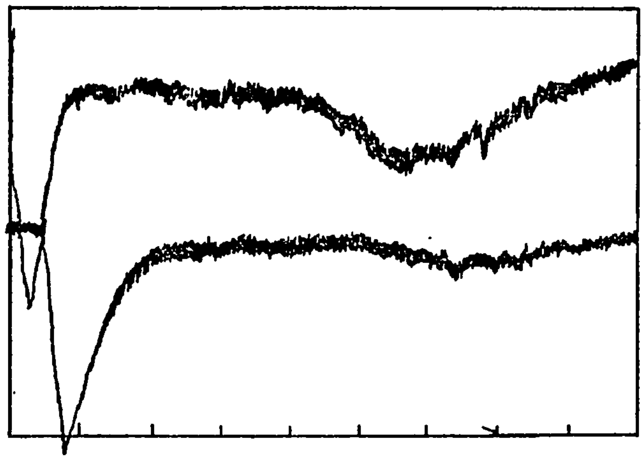

Cylinder
Grounded
500 nsec/cm
.05 v/cm

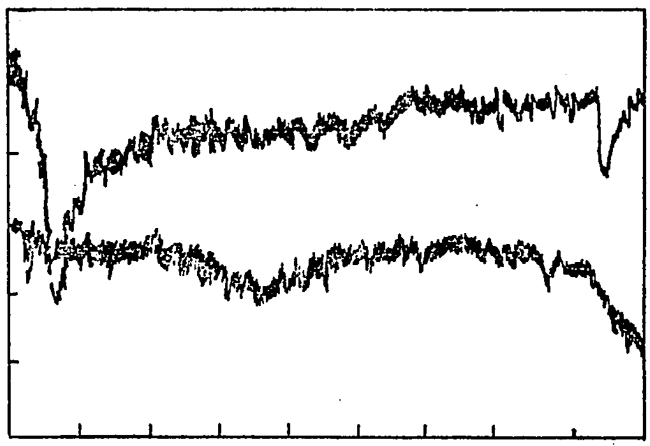

Figure 8. Floating cylinder vs. grounded cylinder.

propagating from electrode to electrode. This kind of breakdown wave surely exists in all electrical shock tubes regardless of circuitry.

The ground system on the shock tube consisted of a six inch metal mechanical connection from the capacitor to the wall of the shielding chamber which was connected to the room ground. It was decided that the shock tube would be reconstructed to eliminate any ground loops so that it might be determined whether or not the wave was sensitive to grounding variations.

The problem was simply to eliminate the ground strap between the electrode and the shielding chamber. This was accomplished by making one electrode an integral part of one wall of the shielding chamber. A three inch hole, large enough to allow the passage of the expansion chamber, was machined in the chamber wall. An aluminum collar was then heat fitted to the electrode and this the was welded securely to the chamber. The expansion chamber, alumina spacer, and other electrode could then be easily bolted to the chamber wall. Figure 9 shows the details of this construction. It should be mentioned that the only change introduced in this reconstruction was the elimination of the six inch metal ground strap. All other parameters of the discharge circuit remained unchanged.

Upon completion of this modification, it was discovered that the wave precursor no longer existed. It was not simply a matter of observing subtle differences in wave speeds, etc., but it was, instead, a matter of observing no wave at all. The true identity of the wave was now clearly exposed. The precursor wave is a breakdown wave in the sense that it is driven by one driver electrode which is suddenly raised

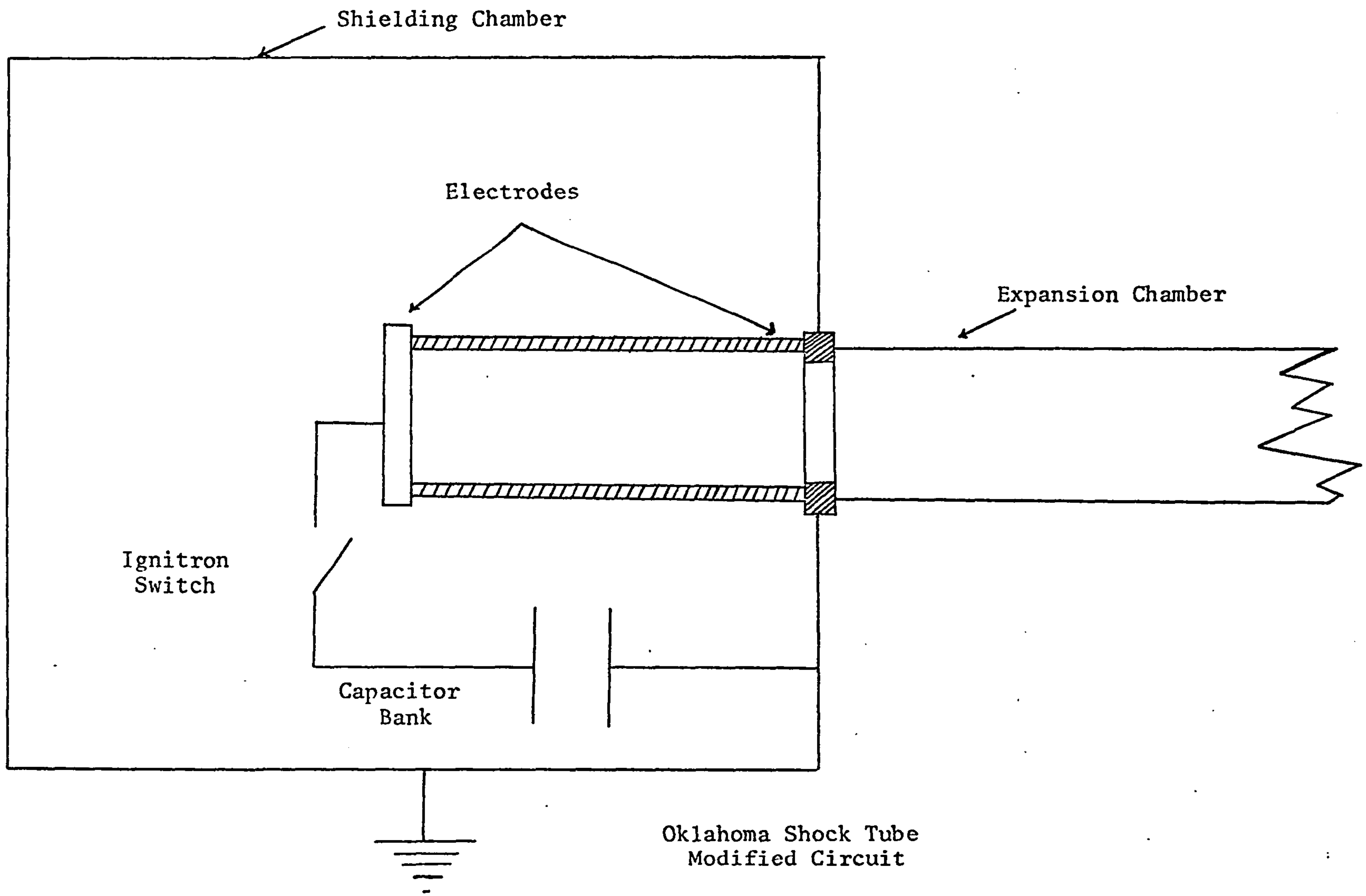

Figure 9. The modified discharge circuit.

to a high potential with respect to infinity. This allows a breakdown wave to propagate in the standard manner. The qualitative explanation of breakdown wave propagation offered by Beams in 1930 still is an excellent source to refer to. The breakdown wave in an electrical shock tube is not, however, a typical breakdown wave which is driven by the potential applied to a capacitor. The wave in this apparatus is driven by the large potential which can be generated across inductances subject to the very large rate of current change (10^{11} amperes/sec) that is developed during the onset of the driver discharge.

The outer electrode, which becomes the driving electrode for the wave, gets its potential by mutual inductance with respect to ground due to the large EMF generated by the changing magnetic flux which links the circuit formed by the electrode, mechanical ground strap, and shielding chamber wall. The strength of the driving potential responsible for the propagation of the breakdown wave depends on the value of the mutual inductance and is thus directly related to the geometry of the discharge circuit.

The existence of the very large current rate of change during the driver discharge is responsible for the induced electron which equals $-M_{AB}\ dI_A/dt$ where M_{AB} is the mutual inductance of the two circuits, marked A and B in Fig. 10, and dI_A/dt is the rate of current change in the discharge circuit A. The negative sign comes from Lenz' [1] Law.

The induced electromotance, responsible for driving the precursor, can easily be calculated if the values of dI/dt and also the value of the mutual inductance, M, of the circuit are known. In the present

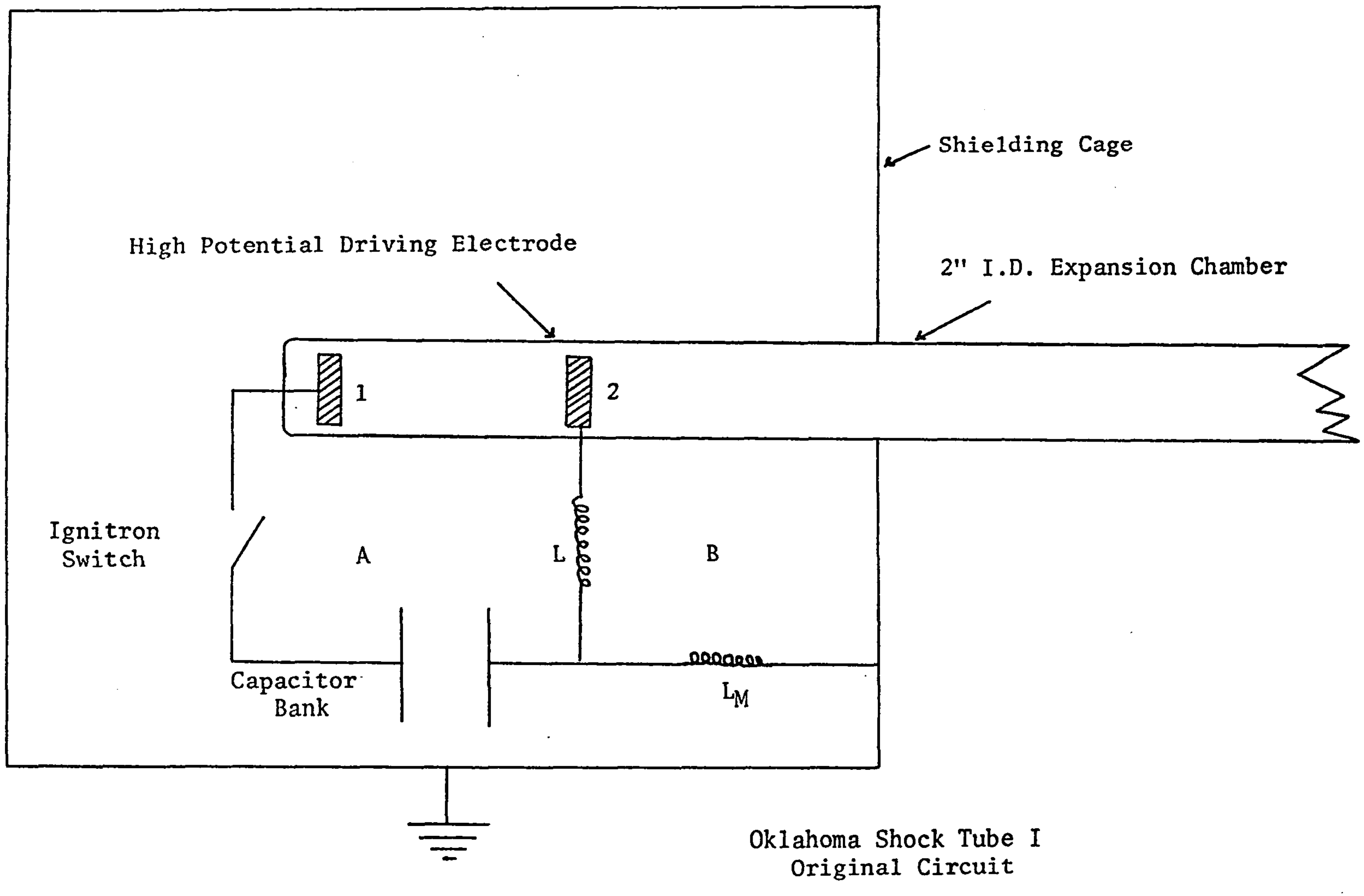

Figure 10. Breakdown wave driving circuit.

shock tube, dI/dt can approach 10^{11} amperes/sec and thus it is seen that an induced EMF of 15,000 volts is capable of being produced for a value of mutual inductance corresponding to only 0.15×10^{-6} henries.

The exact behavior of dI/dt in the shock tube is difficult to analyze. The analysis by Fowler [25] of the discharge data of several electrical shock tubes indicates that the driver is a non-linear resistive element which may be approximated by the expression

$$R = R_o e^{-kt} + V_{capacitor}/I \ .$$

This indicates that the current and voltage may well display non-ohmic characteristics until the gas in the discharge driver becomes highly conducting. This non-ohmic behavior would alter the behavior of the dI/dt and also the behavior of the driving voltage induced. Such an alteration would affect the launching of the precursor.

With the nature of the wave precursor now clear, it was decided to continue investigations on this new arrangement in order to determine whether or not residual components, which might be responsible for any precursive effects, existed.

Two minor phenomena were found to exist although neither would explain the descrepancies between fluid dynamical prediction and experiment that have been observed in the electrical shock tube. These two residual components will be discussed below.

Photopreionization

There did exist in the new apparatus some photo-excitation or ionization during the first microsecond or so of the electric discharge driving the shock tube. This luminosity did not change appreciably when switching from one discharge circuit configuration to another. This luminosity was, however, affected greatly by impurity concentrations in the gas. The phenomenon had no distinct optical profile and manifested itself only as bright radiation which appeared to follow the capacitor oscillations and which progressed at light speed.

Observations made of the attenuation of this photoionization in conditions of great purity indicate a $1/r^2$ dependence. The results implied that one could begin to study the precursor, free from any photoionization contribution, at a point approximately fifty centimeters from the driver when using the original circuitry.

Another interesting aspect of this photon induced luminosity was discovered during electron temperature measurements taken on the main expansion chamber. Russell predicted that if photon absorption were a major mechanism producing near-driver, hot precursive electrons then one would expect that in the vicinity of the driver the temperature would increase with distance since the higher energy photons would go further due to the photoionization cross section decreasing with increasing energy. This was not found to be the case in this apparatus.

Electron Diffusion

Extensive studies were also made in the side arm of the modified shock tube in an attempt to observe any existing luminosity in advance of the plasma acoustic shock.

One observation station was established employing the RCA 7746 PM. This very sensitive tube was operated at the maximum anode-cathode supply voltage of 2,500 volts. The signals were fed into the type 454 oscilloscope and compared to the discharge current dI/dt. The station was mounted 300 cm from the driver.

A very low intensity, diffused, optical signal appeared some five microseconds after the onset of the driver current. The face of the 7746 was then covered in order to distinguish real signal from PM noise. All trace of a signal vanished when this was done. The ends of the meter long sections of pipe forming the side arm and expansion chamber were baffled using brass rings to prevent light originating in the vicinity of the driver from being piped down the walls of the tube. This had no effect on the signal observed.

Our final conclusion is that this phenomenon involves the diffusion of electrons similar to the effect first observed by Weymann. It is not apparent that this luminosity should be called a front due to the apparent lack of a sufficiently rapid rise in electron concentration. The densities and temperature associated with the electron diffusion as observed in the apparatus are negligible when compared to the precursor wave's contribution.

The remainder of this work will focus on the detailed study of the induction driven breakdown wave which constitutes the major component of precursive effects in the electrical shock tube.

Experimental Studies of the Induction Driven Breakdown Precursor

Studies of the precursor were made of waves driven by both positive and negative polarities. Shelton introduced the terms proforce waves, for which the electric field accelerates the electrons in the direction of wave propagation, and antiforce waves for the case where electron acceleration and wave propagation are opposite directions. The former case arises when the driving electrode is negative with respect to ground and the latter when the electrode is positive. Referring again to Fig. 10, it can be seen that if the floating electrode (#1) of the driver section is pulsed positively, then the induced electromotance is such that electrode number 2 becomes positive with respect to ground, thus generating antiforce waves. When electrode number 1 is pulsed negatively then electrode number 2 becomes negative with respect to ground and proforce waves are propagated.

The connection of the power supply, capacitor, ignitron switch, and driver in the proper sequence allows one to study proforce or antiforce waves at will. Figure 11 is a block diagram demonstrating the circuitry for both proforce and antiforce waves. The ignitron must be maintained in a fixed vertical position and it will pass current in only one direction. These facts must be considered when the polarity change is made.

The Effect of Heat Conduction

Fowler and Hood had postulated that the very hot electron gas existing in the shock tube driver after the initiation of the discharge might provide an energy source for precursive effects. Energy could be transmitted to the wave front by heat conduction via electron-electron collisions. Although the result with the modified circuit of Fig. 9 had shown that this could not be the principal process responsible for the precursor, it was anticipated that such an effect might still augment the wave. To test this postulate, the following experiment was conducted.

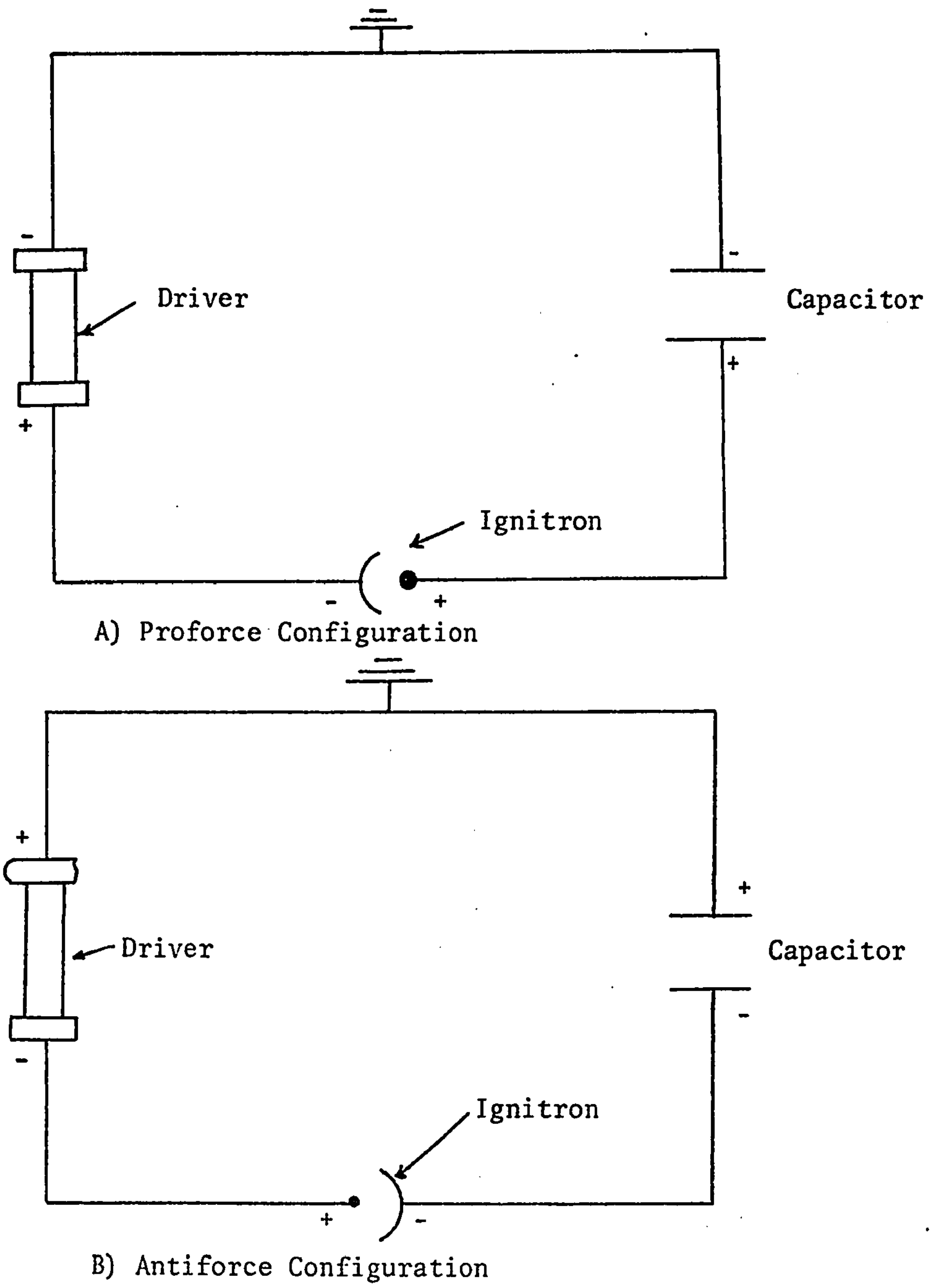

Figure 11. Proforce circuit vs. antiforce circuit.

A one-half inch thick brass plate, two inches in diameter, was machined so that it could be pressed tightly into the cylindrical electrode of the driver. Once in place, the driver was completely closed while the discharge circuitry of the shock tube was not affected. In this way none of the hot driver gas could escape into the expansion chamber but the breakdown wave precursor would still be launched and propagated. In analyzing the results, it was assumed that no photo-ionization effects significantly aided the precursor. Such an assumption seems experimentally justified. Also, all measurements were made in the side arm.

The plugged driver resulted in a decrease of both the velocity and intensity of the wave. It is concluded that the breakdown wave precursor is augmented by what is most likely heat conduction from the driver.

Wave Speed Studies

Wave speed studies of the precursor were made of both proforce and antiforce waves utilizing the same techniques. The wave speeds were obtained by measuring the time of flight of the wave for several viewing slots along the discharge tube. Ten centimeter long cylinders of black paper were used to form the slots. The width and effective height of each slit were adjusted during operation to insure that signals of near constant amplitude, at one value of PM voltage, could be obtained during an entire run. This avoided the need to progress from low to high PM operating voltages which would affect the time response of the tube. Signals were recorded on a dual-beam oscilloscope triggered externally by a 931-A PM stationed fifty centimeters downstream from the driver.

The EMI 9558 and the RCA 7746 recorded the wave's passage. Figure 12 shows a block diagram of the experimental apparatus.

The experimental procedure was to position the EMI 9558 at a fixed location and then move the RCA 7746 to viewpoints progressively further downstream. The time of flight, t, of the wave was then measured between two viewports and the average velocity between these two points was calculated as v = t/L where L was the distance travelled by the wave. Measurements were taken at ten centimeter intervals from a position about fifty centimeters downstream from the driver to the point where the wave would abruptly cease to propagate. This abrupt cut-off will be discussed later.

The sharp profile of the wave together with the very rapid rise time of the optical profile allowed accurate monitoring of the time intervals involved. The time of flight was measured by taking the time difference from the onset of the wave at one station to the onset at a second station.

The above method, owing to the sharp optical profiles, fast risetimes, and great reproducibility of the wave launching apparatus, was trusted to produce accurate results. A second technique, however, was used to check the velocity results for accuracy. This method is discussed in detail in the dissertation of R. N. Blais [26] and offers higher absolute time resolution than any known method of wave speed analysis. The method makes use of nuclear data handling techniques and basically is as follows.

Two PM tubes were positioned before the viewports and the PM signals were applied by times cables to the start and stop inputs of

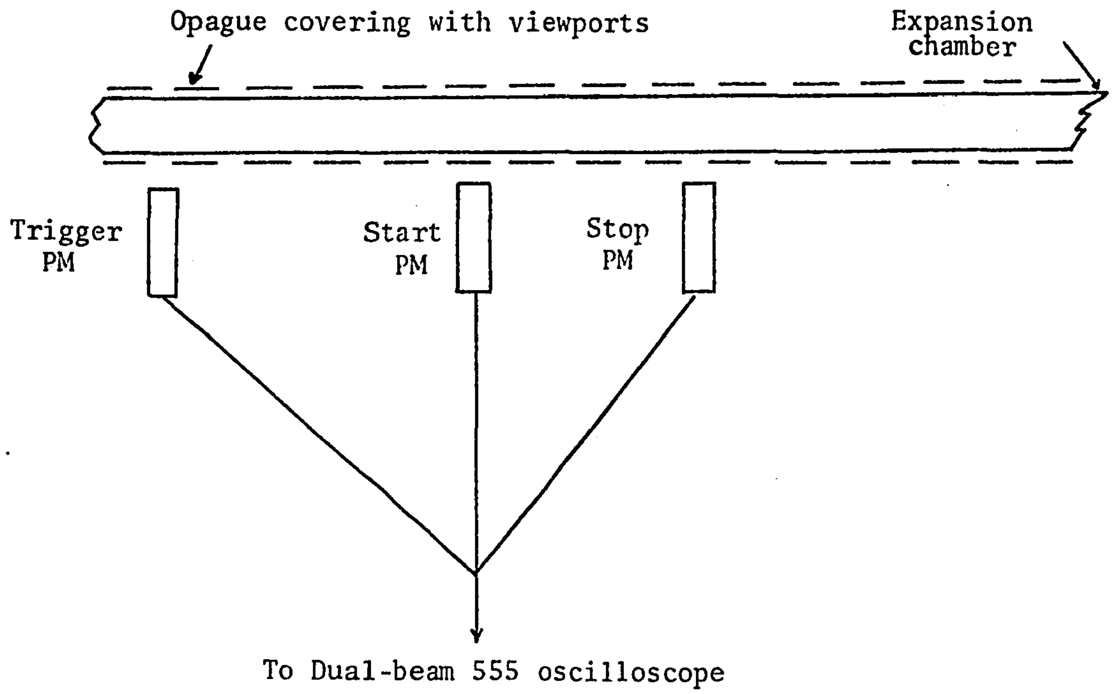

Note: Stop PM may be replaced with monochromator. All PM's on moveable carts mounted on rails.

Schematic of wave speed measuring system.

Figure 12. Block diagram of wave speed measuring system.

a time to pulse height converter. The output pulse was voltage analyzed by a multichannel analyzer which could assemble and store the results of a statistically significant number of events. Data on time delays between observation ports were read out on an oscilloscope. The entire apparatus could be calibrated against delay lines known to about one nanosecond. The procedure was to leave the start PM at a fixed position along the tube and to move the stop PM to a successive ports, obtaining distance versus time plot and thus the velocity of wave as a function of distance.

This statistical method of wave speed measurement was used to measure the precursor wave speeds for a few values of E and P and the results were then compared to those results obtained at the same values of E and P by the oscilloscope method described above. In all cases the relative error between the two was not significantly greater than one per cent. The reason for this agreement of course is due to the rapid risetime and very constant behavior exhibited by the precursor in our apparatus.

One further consideration is necessary before listing the experimental results. The voltage driving the wave, and therefore parameters such as wave speeds and temperatures, all depend directly on the value of the mutual inductance of the discharge circuit. It has been previously mentioned that this value depends only on the geometry of the circuit. Therefore the results below will be valid only for one particular value of mutual inductance, although the linear dependence of driving voltage to mutual inductance would allow one to extrapolate the results to other cases. It was observed experimentally that changes in the connecting elements of the discharge circuit had a direct effect on the wave's parameters. An effort was made to make the connections of the various elements of the discharge circuit as short as mechanically possible. Inductive loops were also eliminated where possible.

The critical importance of the discharge configuration on the wave's performance introduces another subtle consideration into the wave analysis. The mechanical changes needed to switch from proforce waves to antiforce waves render it very difficult to study both kinds of waves under identical conditions. An attempt was made to tailor the circuits so that the parameters were approximately the same in both cases. It should be mentioned that the observations of Isler and Kerr [27], who observed a precursor under only one polarity, were probably the result of a great lack of parity in the values of circuit inductance for the two cases. A very small value of circuit inductance would result in the generation of a weak precursor or, in the extreme case, no wave at all.

Velocity vs. Distance. The wave speed data was plotted as a function of distance and the results for waves of both polarity appear in Figs. 13 and 14. The fact that these plots are linear on log-log paper indicates that the wave speed follows a power law decay curve with respect to distance. Specifically, the precursor wave speeds appear to depend on distance about like

$$v = \beta Z^{-1} .$$

One could perhaps have a clearer picture of the waves attenuation if the expression relating v with z is differentiated with respect to z. This operation gives

$$\frac{dv}{dz} = - \beta z^{-2} .$$

It should be noted that the actual slope of the v vs. z graph is greater than one and is actually closer to 1.1. 1.1 represents the slope of the least square fit of the data points. There are actually two slopes involved. One slope, slightly less than one, is applicable to a line drawn through only those data points obtained in the main expansion chamber. Another slope, slightly greater than one is obtained from the data taken in the side arm.

The greater attenuation of the wave speeds in the side arm is most likely due to the fact that the heat conduction process feeding energy to the front must act along two different paths for waves propagating in the side arm. There may also be a slight viscous effect imposed upon the wave by the junction between the side arm and the main expansion tube.

If one assumes that the wave is, in general, governed by the expression $dv/dz = - \beta \bar{v}^2$, then it is clear that the constant β must have the units of cm^2/sec. These units are proper for a diffusion constant and it is postulated that the attenuation of the precursor is a result of the diffusion of electrons in a radial direction resulting in energy loss through heat conduction.

It would prove interesting to carry out a more extensive analysis of the constant β in order to exactly realize the nature of the processes governing the attenuation of a breakdown wave of the precursor's complexity.

One more feature of the results of the velocity as a function of distance studies remains to be discussed. It was observed that the wave abruptly ceased to propagate after traveling some critical distance z where z depended on the applied capacitor voltage, V, and the gas pressure, p. In a ten centimeter interval the optical intensity of the wave could drop from its full value to a negligible amount. This effect is easily understood by once again studying Fig. 10. The wave will propagate as long as a voltage, with respect to infinity, remains on the ground electrode. The sudden termination of the precursor results from the plasma acoustic shock wave traveling the ten centimeter distance from the electrode to the orifice in the sheild box, and thus shorting out the manual inductance that maintained the driving potential. The wave will accomplish this shorting in a shorter period of time than is required for dI/dt to go to zero. It was found that the termination distances observed required that the plasma acoustic shock wave be traveling with speeds of from 10^6 to 10^7 cm/sec, depending on the applied capacitor voltage V and the gas pressure p. These speeds agree with the experimental values observed on this shock tube.

The observation of the cut off and the reason behind such a termination emphasizes the very critical nature of distance between the ring electrode and the orifice. Assuming plasma acoustic shock wave speeds of 10^7 cm/sec implies that for a ten centimeter distance between electrode and orifice, as exists in the present apparatus, a precursor might be propagated for one microsecond while for a distance of two centimeters, the wave would be terminated after only two-tenths of a microsecond. For a precursor whose wave speed is 5×10^8 cm/sec, the former condition results in a five member propagation distance while the latter case implies a propagation of only one meter.

Finally it should be emphasized that the results given above for proforce and antiforce waves were not taken under the exact same conditions for each case. Comparisons, therefore, of the two kinds of waves based on the data presented should be made with caution. It should be mentioned, however, that proforce wave speeds appear to be faster than antiforce wave speeds. This observation was also made by Blais.

Wave Speeds as a Function of V and p. The dependence upon wave speeds as a function of the applied capacitor voltage V and gas pressure p was also studied.

The results of the study of the wave speed dependence on the voltage applied to the capacitor are given, for both the proforce and antiforce case, in Figs. 15 and 16. These results deserve some comment.

The voltage applied to the capacitor of the shock tube and the voltage actually driving the precursor breakdown wave do not have the same value. Only a fraction of the capacitor voltage is induced between the ring electrode and ground. This fraction, as has been previously mentioned, depends only on dI/dt and the geometry of the discharge circuit. A low impedance voltage driver was used to give an indication of the magnitudes of the induced voltages and results appear in Fig. 17.

Finally, it should be mentioned that the results of wave speed as a function of applied capacitor voltage apply only to one discharge circuit geometry. One would get different results for different geometries

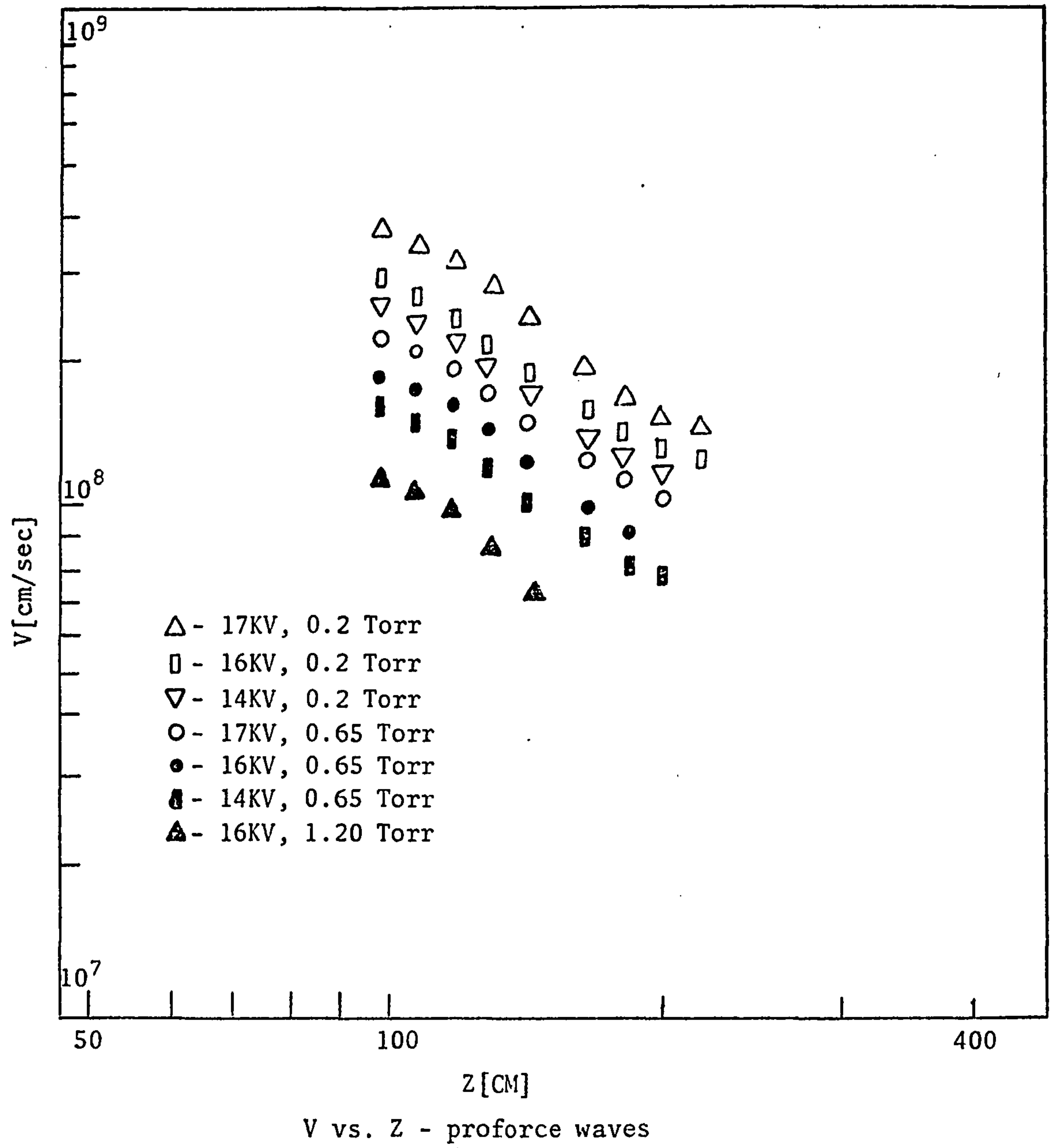

Figure 13. Wave speed vs. distance for a proforce wave.

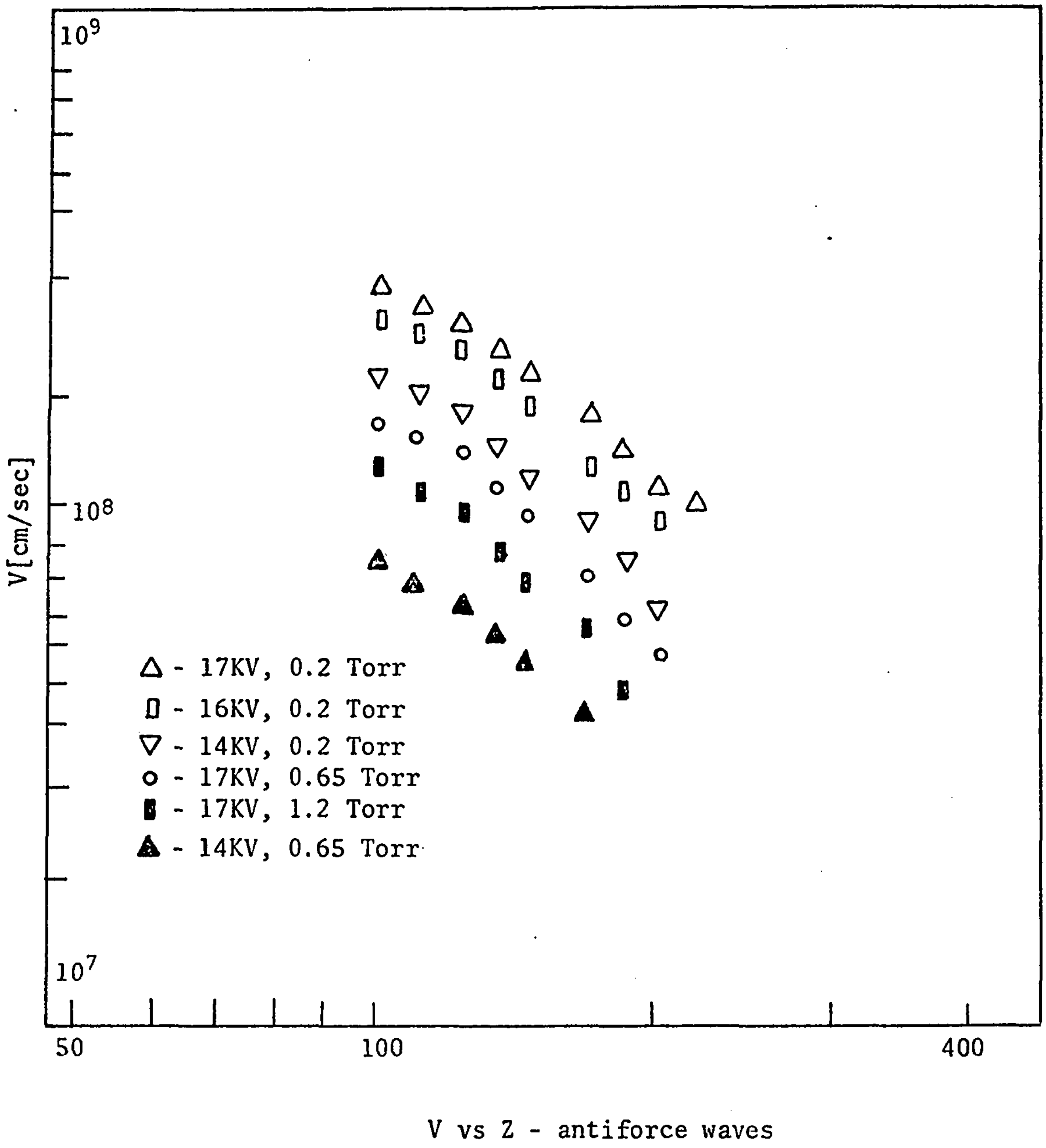

Figure 14. Wave speed vs. distance for an antiforce wave.

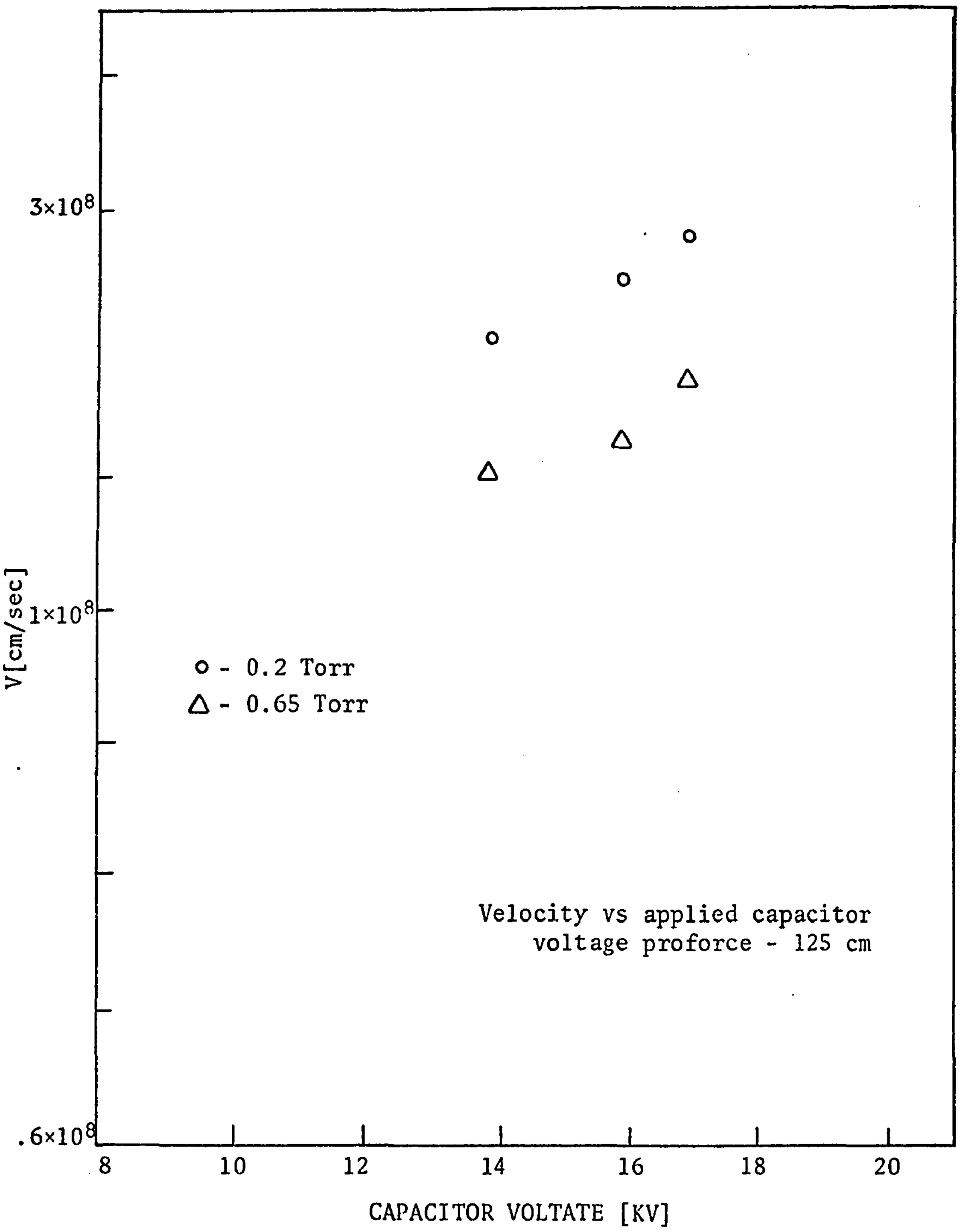

Figure 15. Wave speed vs. applied capacitor voltage for a proforce wave.

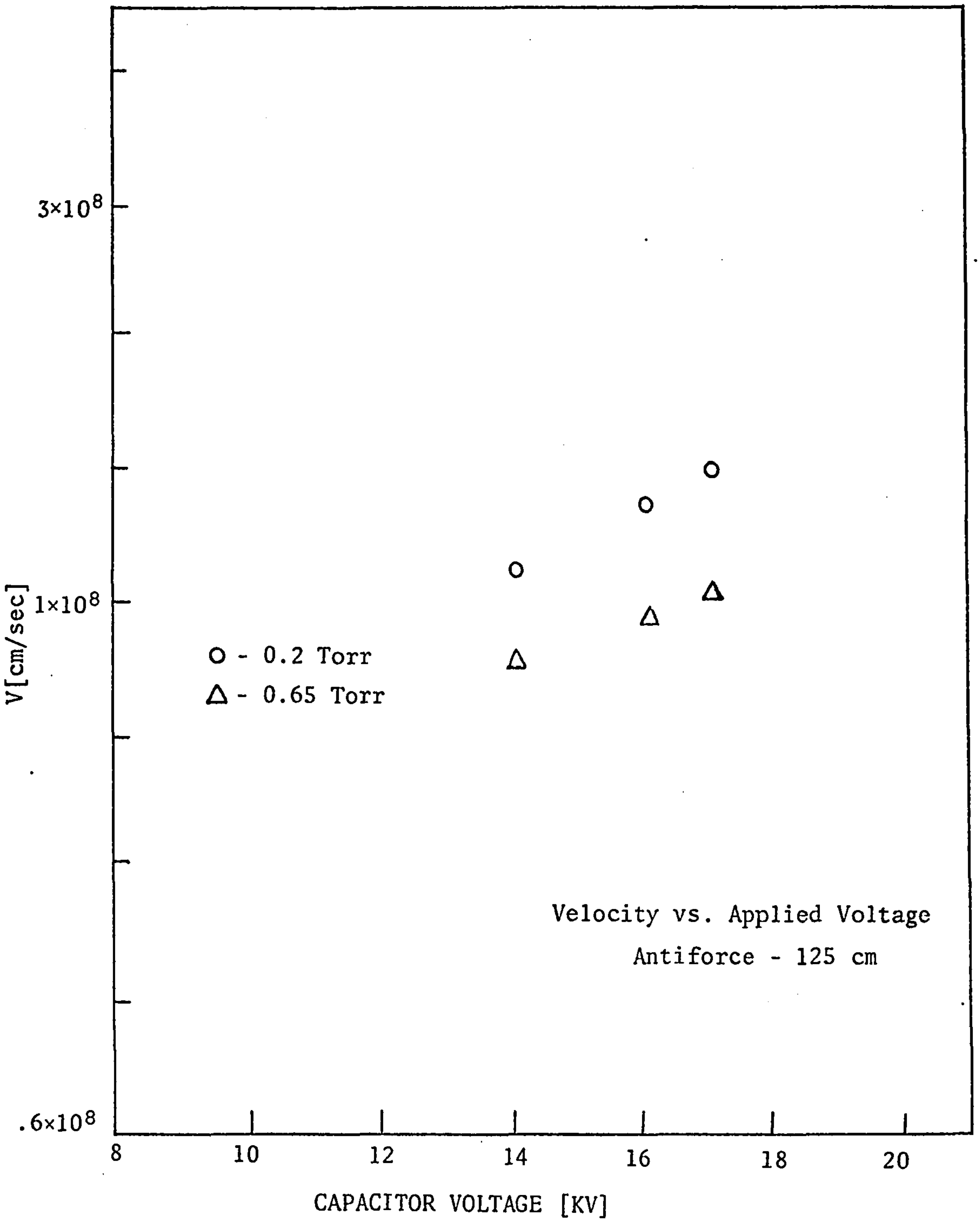

Figure 16. Wave speed vs. applied capacitor voltage for an antiforce wave.

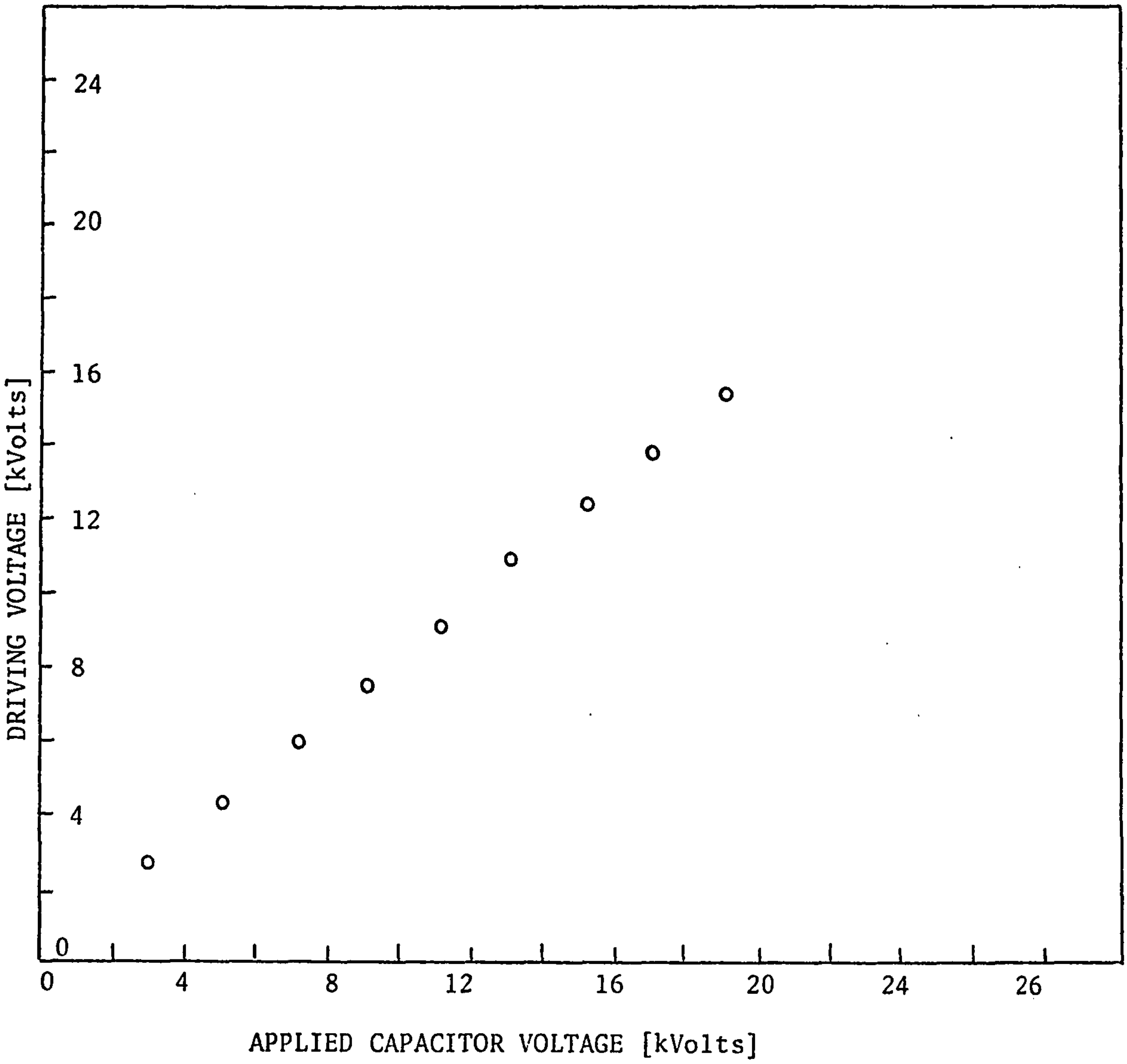

Figure 17. Applied voltage vs. driving voltage.

even though the value of applied voltage were held constant. This should be remembered when comparing this data to the results obtained on a different apparatus.

Velocity as a function of gas pressure was also studied. Pressures ranged from 0.2 torr to 2 torr. Results for both proforce and antiforce waves are shown in Figs. 18 and 19.

One can see from these figures that the wave velocity is related to the gas pressure as

$$v = kp^{-\frac{1}{2}} .$$

Finally, the axial electric field probes discussed earlier were used to measure the axial electric field appearing at the front and wave velocity as a function of electric field, E, was studied. These probes in reality measure the space charge field resulting from the electron mobility. This space charge field perturbs the potential distribution at the front and tends to nulify the applied electric field thus allowing the field to gradually go to zero in the ionized gas behind the front. More will be said about the axial electric field operating in the shock tube.

The data was plotted as wave speed against E/p and the results were compared to the values predicted by Shelton; such agreement should not be expected in the case of the shock tube precursor breakdown wave. Shelton uses a three fluid model to analyze the case of one dimensional waves traveling in the direction an electron would be accelerated by the applied electric field. Such an analysis should describe a proforce precursor with no augmentation. The precursor, however, receives additional energy through heat conduction. It is anticipated that the

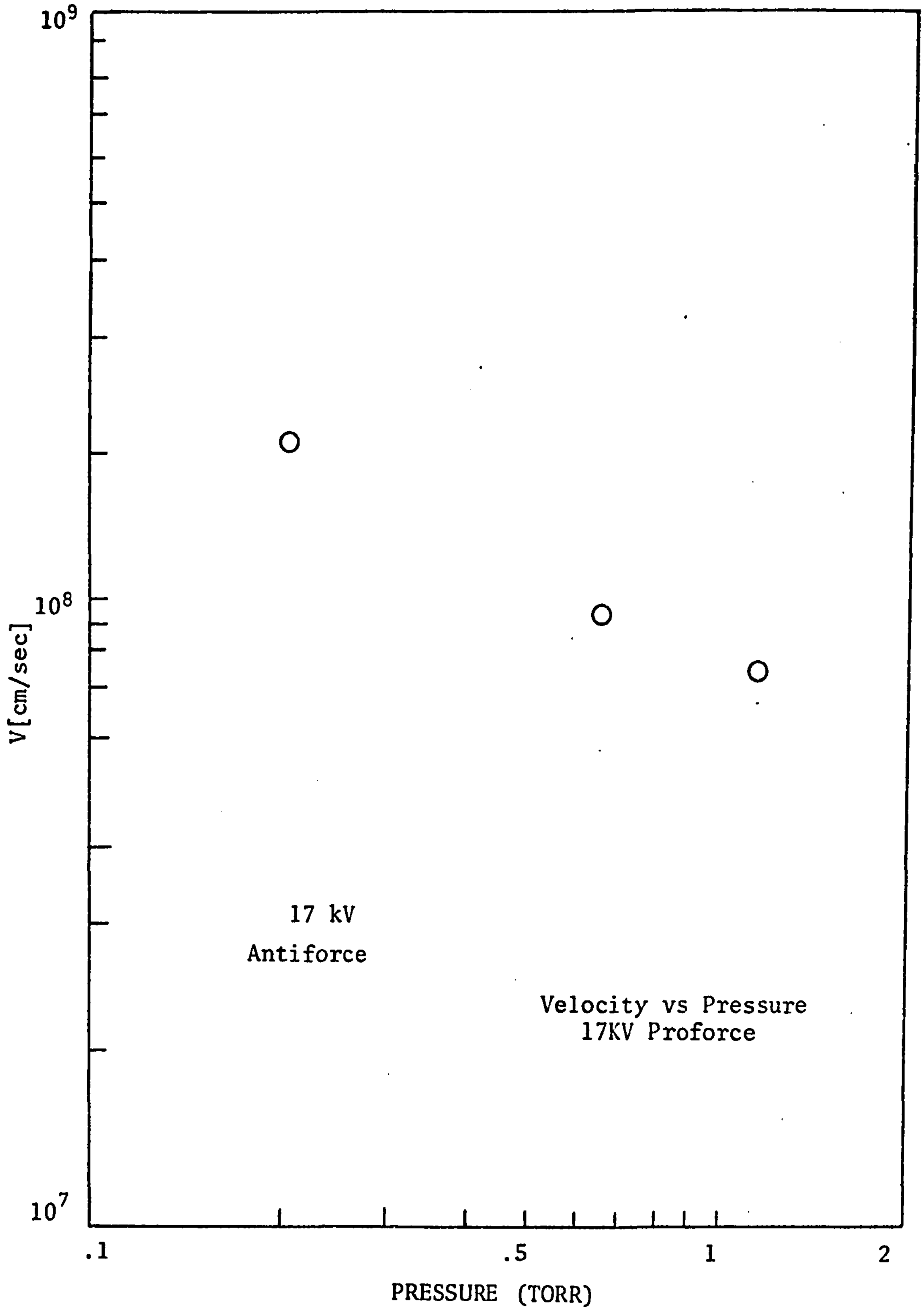

Figure 18. Wave speed vs gas pressure for a proforce wave.

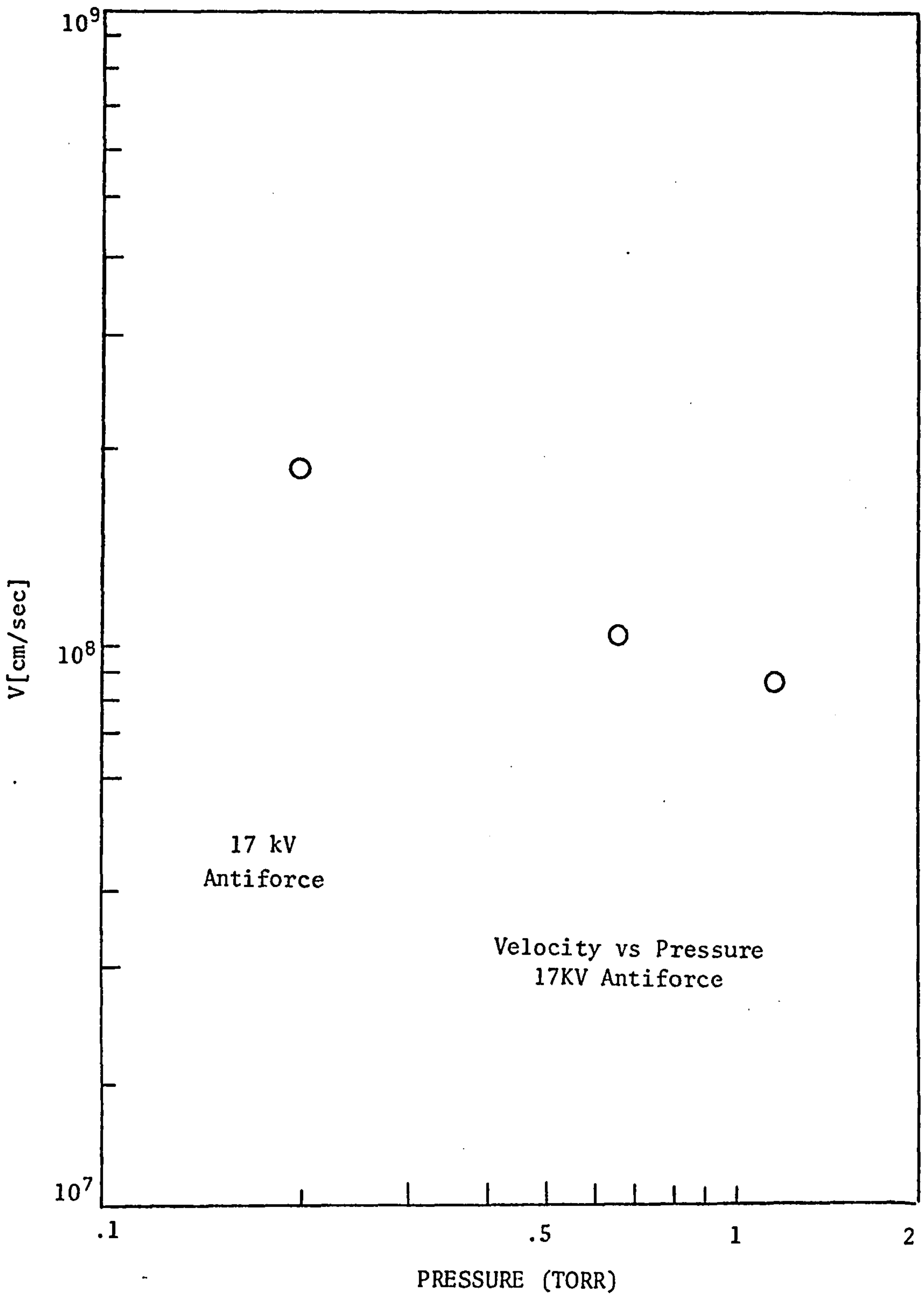

Figure 19. Wave speed vs. gas pressure for an antiforce wave.

addition of an appropriate hot electron chemical potential in Shelton's equations would result in an analysis more descriptive of the shock tube precursor.

Electron Temperature and Density Measurements

Discussion of the Method

The electron temperatures and densities were measured using the Jarrell-Ash monochromator and the RCA 7746 PM, both having been previously described. The monochromator-PM system was mounted on a movable cart and could be moved along the rail, parallel to the tube, to any desired viewport. The EMI 9558 PM was used as a stationary trigger to activate the horizontal sweep of the 454 oscilloscope. Results were recorded by a Polaroid camera mounted on the oscilloscope. The electron temperatures and densities for waves of both polarity were measured using this apparatus.

The method used to measure the temperatures and densities is based on the technique described by Latimer, Mills and Day, but involves the analysis of a time varying case rather than a static one. The method is derived from the following considerations.

If the excitation of the gas atoms in a tenuous helium plasma is assumed to be due solely to electron collisions, and multiple processes such as excitation transfer or excitation from the metastable states are assumed to be negligible, then the intensity as measured by a photomultiplier tube, of a spectral line involving a j to k transition is given by

$$I_{jk} = f_{jk} J_{jk} / h\nu_{jk}$$

where F_{jk} is a constant depending on the spectral response of the PM and the optical parameters of the system being studied, H_{jk} represents the energy of the photon released, and J_{jk} is defined as

$$J_{jk} = A_{jk} n_j h\nu_{jk}$$

where A_{jk} is the transition probability and n_j is the number of atoms in the jth excited state.

For the non-steady state one is interested in dI/dt and the expression can be written as $\frac{I}{A_{jk} f_{jk}} \frac{dI}{dt} = - \frac{i}{f_{jk}} + (\sigma_{jk} v) N n_e$ where $(\sigma_j v)$ represents the optical cross sections for the jth level multiplied by the electron velocity and averaged over the plasma electron velocity distribution, and N and n_e represent the number of neutral atoms and the number of electrons respectively. By dividing the above equation by a similar one for a different transition we have

$$\frac{1/A_{jk} f_{jk}\ dI/dt + I/f_{jk}}{1/A_{\ell m} f_{\ell m}\ dI/dt + I/f_{\ell m}} = \frac{<\sigma_{jk} v>}{<\sigma_{\ell m} v>} \qquad (1)$$

Thus we have on the right hand side of Eq. (1) the ratio of two cross sections which are different functions of electron velocity and therefore a variable function of electron temperature. The two cross sections, it should be stressed, must have a different functional dependence on the electron temperature. For this reason one might compare a singlet to a triplet transition for example. The left hand side of the equation can be computed once the experimental values of I have been obtained.

Experimentally, the I's were measured in arbitrary units from oscilloscope photographs enlarged via an opaque projector.

Values of I were measured at ten nanosecond intervals along the entire optical profile of the wave. The ratio on the left of Eq. (1) was then computed on an IBM 1130 computer using the program listed in the Appendix. This ratio was compared to the ratios of cross sections tabulated by Latimer, Mills and Day. These tabulated values are found in Table 1.

The above considerations allow one to measure electron temperatures and require only a relative calibration of the optical system. The electron density may also be measured by using the expression $Ne = (I_{jk}/J_{jk} V\ No)$ but requires an absolute calibration. A tungsten ribbon standard lamp was used for this calibration. The calibration was patterned after the method discussed by St. John [28].

The spectral lines chosen for the measurements were the 5048 angstrom He line and the 4713 angstrom He line. These two lines were sufficiently isolated and intense enough to make them easily observable and experimentally quite practical. The choice of these two lines offers an additional advantage. The 5048 line in He originates from the 4^1S level while the 4713 line originates from the 4^3S level. The excitation cross sections of lines originating from these levels have been shown by Miller [29] to be relatively free from pressure effects.

These lines also have the advantage that the radiation from the electron beam cross section measurement experiments is unpolarized and hence the cross sections will be more accurate since no corrections for anisotropy of the emission of radiation are necessary. The actual values of the cross sections used in the calculations were obtained by Latimer [30].

Table I. Maxwellian Averages of Optical Cross Sections for Helium $\langle Q_{jk}v \rangle$ and Calculated Line Ratios as a Function of Electron Temperature (Multiply all averages by 10^{-11}).

kT(eV)	5048Å	4713Å	4438Å	4121Å	4686Å	I_{5048}/I_{4713}	I_{4438}/I_{4121}	I_{4121}/I_{4686}
2.0	8.64E-5	1.66E-4	2.70E-5	4.59E-5	7.93E-18	0.521	0.588	
2.5	8.83E-4	1.62E-3	2.85E-4	4.75E-4	1.71E-14	0.544	0.6	
3.0	4.09E-3	7.29E-3	1.37E-3	2.22E-3	2.90E-12	0.565	0.615	
3.5	1.24E-2	2.11E-2	4.16E-3	6.60E-3	1.15E-10	0.587	0.631	
4.0	2.81E-2	4.63E-2	9.57E-3	1.48E-2	1.82E-9	0.605	0.647	
4.5	5.29E-2	8.46E-2	1.82E-2	2.75E-2	1.58E-8	0.624	0.665	
5.0	8.76E-2	1.36E-1	3.05E-2	4.47E-2	8.89E-8	0.643	0.682	
5.5	1.32E-1	1.99E-1	4.63E-2	6.63E-2	3.68E-7	0.660	0.698	
6.0	1.86E-1	2.73E-1	6.55E-2	9.15E-2	1.21E-6	0.679	0.716	76000
6.5	2.48E-1	3.55E-1	8.77E-2	1.20E-1	3.30E-6	0.697	0.733	36400
7.0	3.16E-1	4.42E-1	1.13E-1	1.50E-1	7.84E-6	0.715	0.75	19100
7.5	3.91E-1	5.33-1	1.40E-1	1.82E-1	1.66E-5	0.731	0.767	10960
8.0	4.70E-1	6.26E-1	1.68E-1	2.15E-1	3.22E-5	0.749	0.784	6670
8.5	5.52E-1	7.19E-1	1.98E-1	2.47E-1	5.77E-5	0.765	0.802	4280
9.0	6.37E-1	8.12E-1	2.29E-1	2.80E-1	9.71E-5	0.784	0.819	2880
9.5	7.23E-1	9.03E-1	2.61E-1	3.12E-1	1.55E-4	0.800	0.836	2070
10.0	8.10E-1	9.91E-1	2.93E-1	3.44E-1	2.36E-4	0.816	0.853	1456
12.0	1.16E0	1.31E0	4.21E-1	4.57E-1	9.04E-4	0.882	0.921	506
14.0	1.49E0	1.56E0	5.43E-1	5.49E-1	2.38E-3	0.955	0.989	230
16.0	1.79E0	1.76E0	6.54E-1	6.19E-1	4.96E-3	1.017	1.057	125.0

Table I (Cont'd.)

kT(ev)	5048A	4713A	4438A	4121A	4684A	I_{5048}/I_{4713}	I_{4438}/I_{4121}	I_{4121}/I_{4686}
18.0	2.06E0	1.90E0	7.55E-1	6.71E-1	8.82E-3	1.084	1.13	76.0
20.0	2.31E0	2.01E0	8.46E-1	7.08E-1	1.40E-2	1.15	1.195	50.4
22.0	2.52E0	2.08E0	9.26E-1	7.33E-1	2.06E-2	1.211	1.26	35.6
25.0	2.81E0	2.14E0	1.03E0	7.55E-1	3.28E-2	1.311	1.366	23.03
30.0	3.19E0	2.15E0	1.17E0	7.62E-1	5.82E-2	1.477	1.54	13.1
35.0	3.49E0	2.12E0	1.28E0	7.48E-1	8.83E-2	1.642	1.71	8.48
40.0	3.73E0	2.06E0	1.37E0	7.26E-1	1.21E-1	1.81	1.885	5.99
45.0	3.92E0	1.98E0	1.44E0	6.99E-1	1.55E-1	1.971	2.056	4.51
50.0	4.07E0	1.90E0	1.49E0	6.71E-1	1.89E-1	2.135	2.226	3.54
55.0	4.20E0	1.83E0	1.54E0	6.43E-1	2.23E-1	2.30	2.394	2.88
60.0	4.31E0	1.75E0	1.56E0	6.16E-1	2.56E-1	2.46	2.56	2.41
65.0	4.41E0	1.68E0	1.61E0	5.92E-1	2.87E-1	2.618	2.72	2.06
70.0	4.48E0	1.62E0	1.64E0	5.68E-1	3.17E-1	2.77	2.884	1.79
75.0	4.55E0	1.55E0	1.66E0	5.46E-1	3.46E-1	2.935	3.042	1.58
80.0	4.61E0	1.50E0	1.68E0	5.26E-1	3.73E-1	3.07	3.2	1.41
85.0	4.66E0	1.44E0	1.70E0	5.07E-1	3.98E-1	3.22	3.35	1.274
90.0	4.70E0	1.39E0	1.71E0	4.89E-1	4.22E-1	3.36	3.5	1.16
95.0	4.73E0	1.35E0	1.73E0	4.73E-1	4.44E-1	3.505	3.65	1.066

Figure 20 shows the measured electron temperature as a function of distance for a proforce wave. Figure 21 shows the measured electron temperature as a function of time along the optical profile of the wave. The maximum values of temperature are listed and these were obtained by using the ratios of the spectral lines at the points on the optical profiles corresponding to ten nanoseconds after the optical onset. Figure 22 shows the measured electron density of a proforce wave as a function of time along the optical profile of the wave.

Figure 23 shows the measured electron temperature of an antiforce wave as a function of gas pressure at a fixed distance along the side arm. Again, these values correspond to maximums.

The results indicate that antiforce waves are hotter than proforce waves and also that the luminous fronts associated with antiforce waves are thicker. This data is felt to be quite accurate within the limits of the time resolution capability of the measuring apparatus. While the data generally agrees with the few measurements of precursor electron temperatures and densities reported in the past, it is lower than the 100 eV temperatures predicted by Shelton for a breakdown wave propagating at 10^9 cm/sec, although at low pressures the electron temperatures approach 70 eV. Larger electron temperatures might be present in a thin sheath at the front and if this be the case then one would require reliable monitoring of the line ratios well within the first ten nanoseconds of the wave's history. It is doubtful, even with an instrument such as the 519 oscilloscope, that such reliability is possible at present.

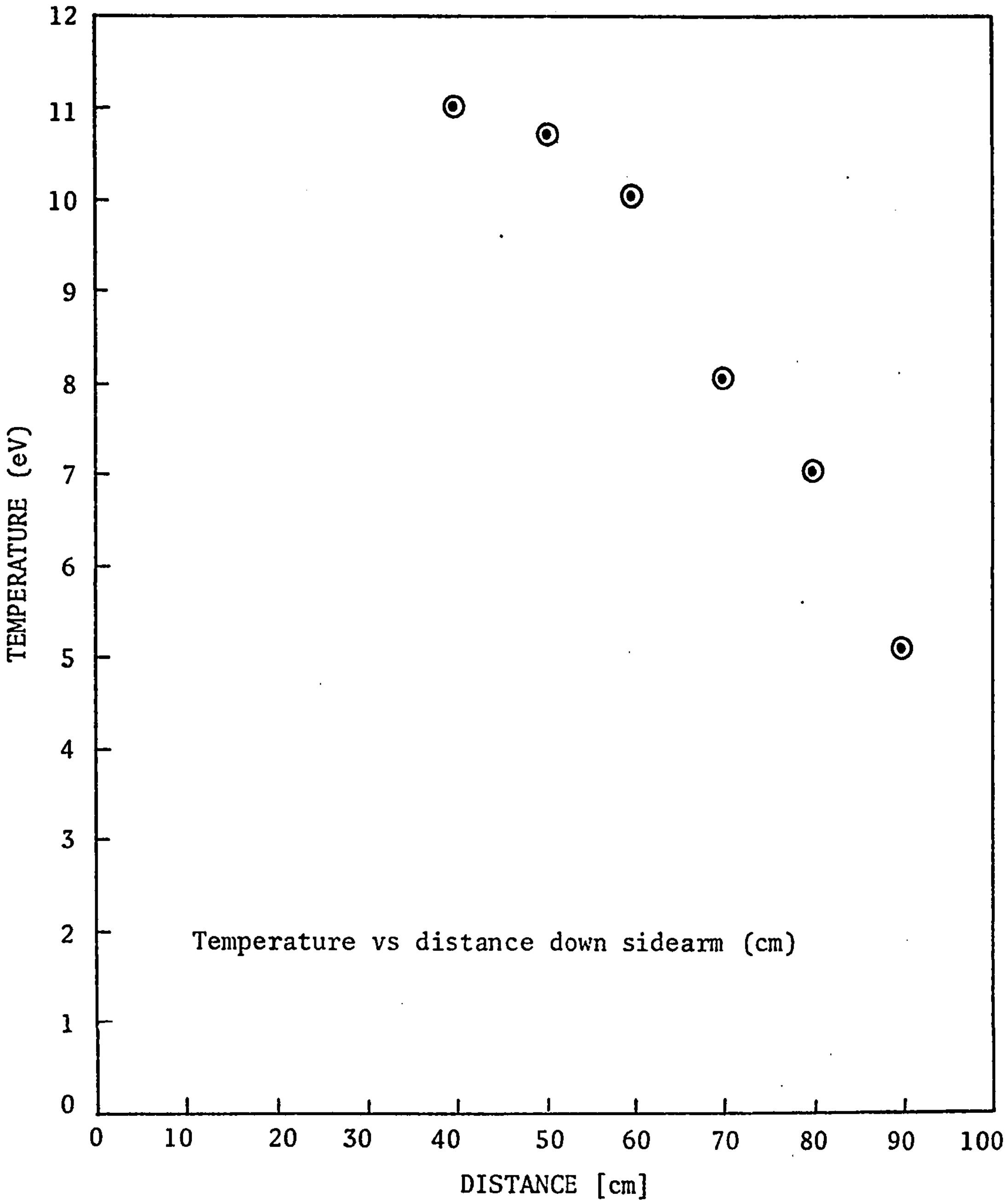

Figure 20. Electron temperature vs. Z for a proforce wave.

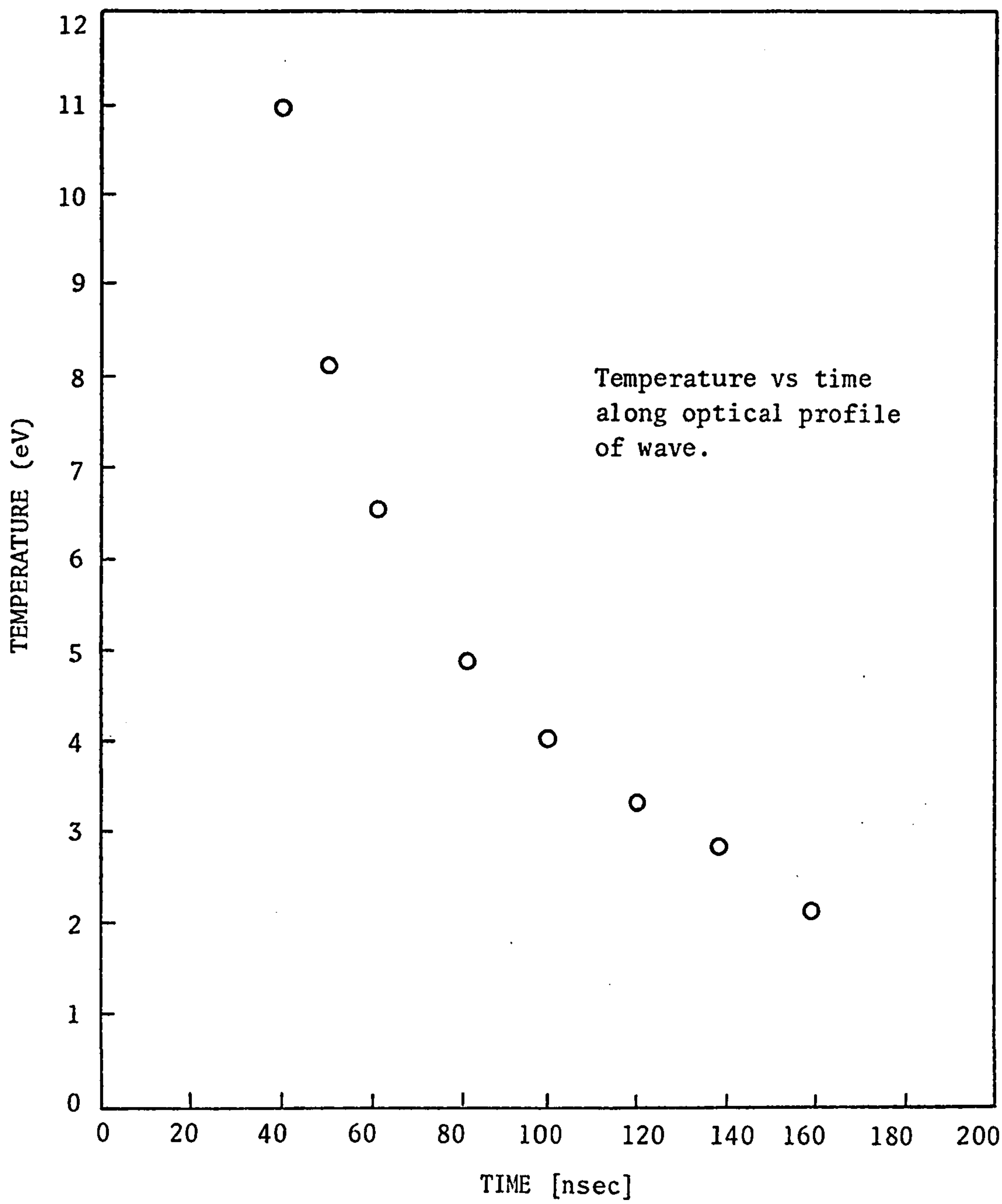

Figure 21. Electron temperature vs. time along optical profile of wave.

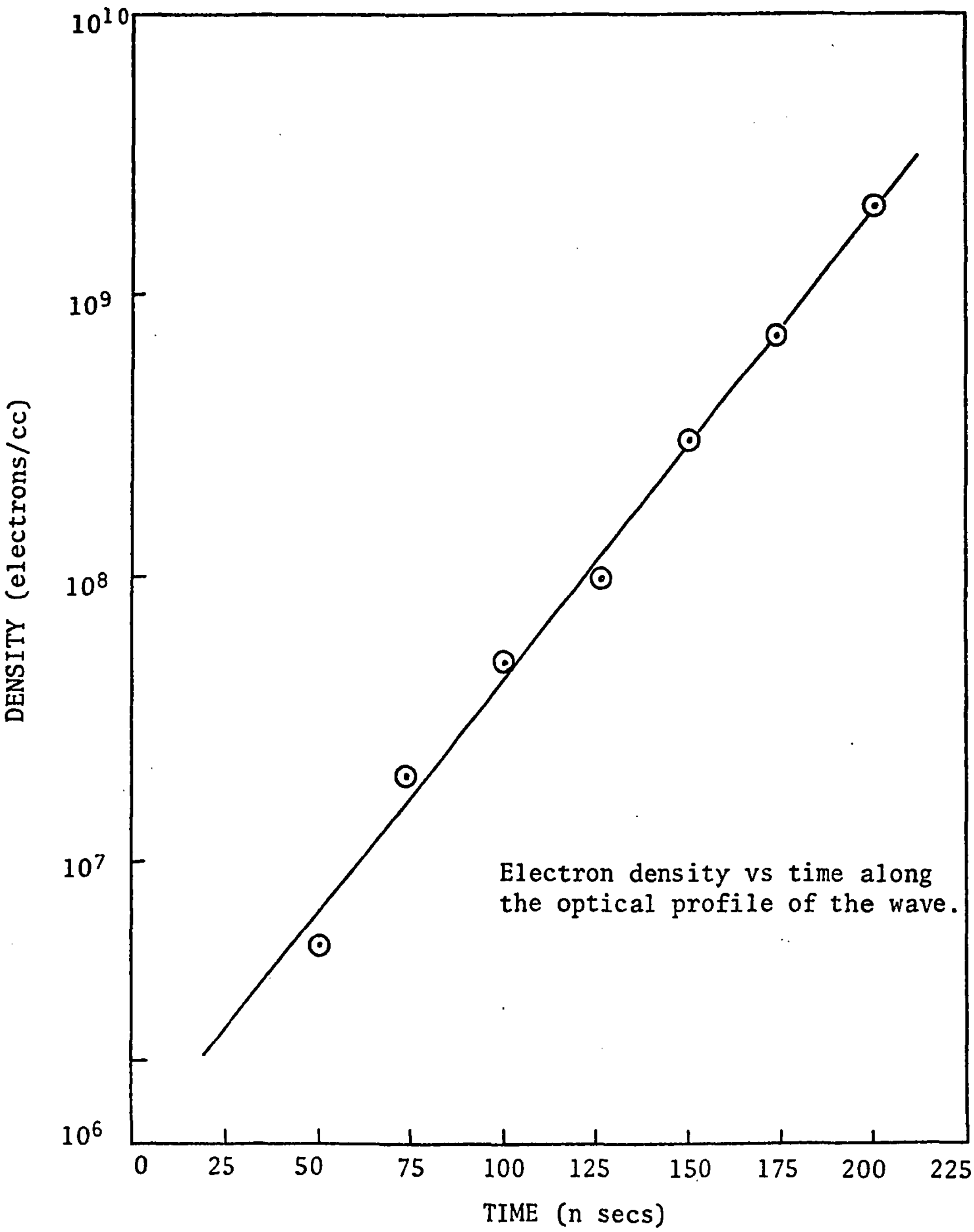

Figure 22. Electron density vs. time for a proforce wave.

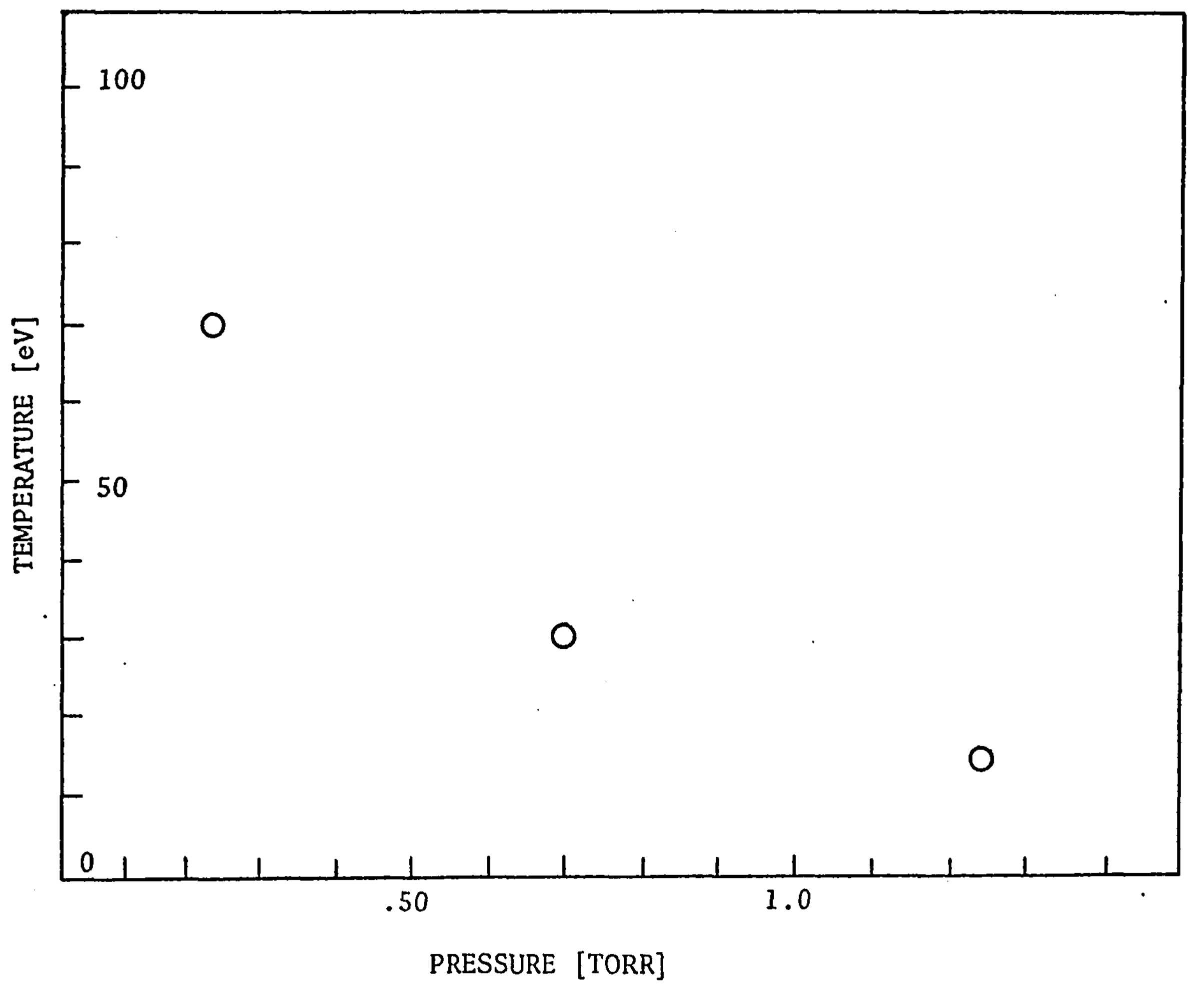

Temperature vs pressure for a fixed position along the sidearm.

Figure 23. Electron temperature vs. gas pressure for an antiforce wave.

The accuracy of the electron temperature measurements as a function of pressure is perhaps questionable. The value of T_e will certainly be quite affected by any pressure dependence of the lifetimes. Also at low pressures, the cross sections if appreciably pressure dependent would be reduced. This would reduce the number of collisions and affect the photon flux observed.

Magnetic Field Studies

The hypothesis that heat conduction might be a major energy transfer mechanism for the precursor prompted the initiation of investigations into the thermal conductivity of the plasma associated with the precursor. The work which will be reported in the balance of this chapter was large initiated and carried out by Dr. M. Naraghi. The author aided Dr. Naraghi in expediting these researches, and is including the results here for record purposes and for completion.

It is well known that a transverse magnetic field has the effect of reducing the flow of heat in a plasma, to a first approximation, by a factor $(1+\omega_{ce}t_c)^{-1}$, where ω_{ce} is the electron cyclotron frequency and t_c is the electron collision time. t_c is about the same for both electron-electron and electron-ion collisions.

To the extent that the precursor relies on heat conduction, the establishment of a transverse magnetic field along the shock tube should increase the heat insulation properties of the gas and thus impede the propagation of the precursor. It was decided, therefore, to carry out an extensive investigation of the precursor's behavior in the presence of a magnetic field in order to clarify the role of heat conduction in the precursor's propagation, to further clarify the nature of the wave, and to provide further information to the important topic of the effect of a transverse magnetic field on thermal conductivity.

In the experiments discussed below, both a transverse and axial magnetic field were utilized. Fringing effects are negligible. The value of the B-field was 2700 Gauss maximum. Assuming an average electron temperature of 10eV for the precursor and a velocity of 10^8 cm/sec, it can be shown that the radius of gyration of the electrons will become smaller than the tube radius. Using the same parameters it can be shown that the electron collision frequency is approximately 6 collisions/an. Therefore at the larger values of magnetic field one can calculate that $\omega\tau \leq 1$. This implies that along one mean free path even one gyration does not take place.

It should be mentioned that in a weakly ionized plasma of the type occurring due to the precursor the great majority of the collisions responsible for the propagation of the wave are those between the neutral particles and charged particles. Because of the relatively small charged particle density (i.e., 10^9 particles cm^{-3}), electron-electron and ion-ion collisions occur much less frequently and make a negligible contribution to the wave propagation. The electrons, however, due to their large mobility at the wave front where a non-equilibrium plasma exists, are more responsible for the collisions than are the ions. Moreover, the electrons in a magnetic field will be more responsible for any effect produced due to the magnetic field owing to their much smaller radius of gyration than the ions.

Velocity and Temperature Effects Due to the Magnetic Field

Figure 24 shows the temperature dependence of the wave due to the magnetic field used upstream. The temperature is measured as a function of the axial distance measured from the onset of the wave.

Figure 25 shows the output of the monochromator with two values of the magnetic field used at the wavelengths. 5048 and 4713Å for helium. Figure 26 shows the delay time observed due to three different values of transverse B-field.

The results indicate that the heat conduction rate was reduced when the magnetic field was increased as expected from theory. In other words the magnetic field enhances the heat insulation property of the gas behind the wave front thus decreasing the effectiveness of the heat conduction process.

The Electromagnetic Induction

The two wire probes, epoxied into a section of pipe, discussed earlier, were used for the electromagnetic induction studies. These studies offered a technique to measure the flow velocity of the wave front. A comparison was made of the results of this study to the previously derived values of the luminous front velocity.

The width of the ionizing wave front is about 15-30 cm long, and of fairly constant speed as shown by the emf induced in it. As the ionized gas flows with a velocity u through the magnetic field of strength B an electric field is produced given by $E = -u \times B$. If the fields are assumed to be uniform and perpendicular to flow velocity, the voltage detected at the terminals is V-uBd.

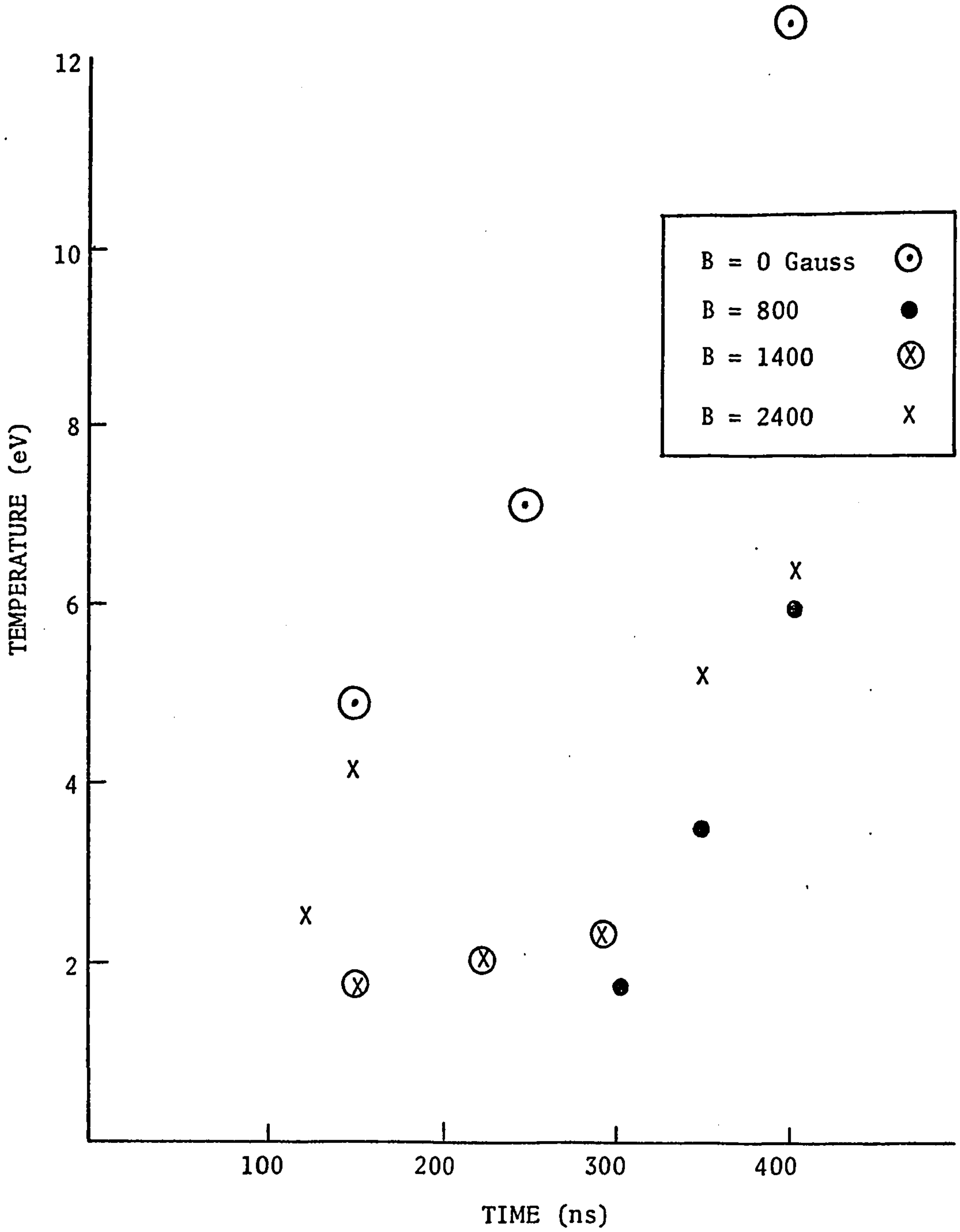

Figure 24. Electron temperature downstream vs. magnetic field upstream.

B = 0 Gauss

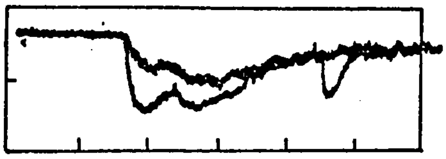

B = 1600 Gauss

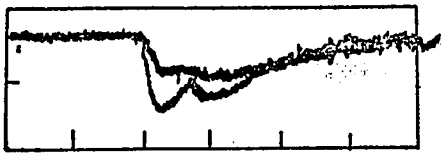

Temperature Measurement

PM tube outputs, $_1$, 5048, and $_2$ = 4713, 500 n/sec per cm

Figure 25. Intensity of 5048 He and 4713 He with two values of Magnetic Field.

500 N sec per cm.

Figure 26. Delay time produced by B = 0, 300, 2100 Gauss.

A typical oscilloscope trace of the voltage detected at the terminals is shown in Fig. 27. A resistance bridge with battery, and in some cases an isolation transformer, was used to isolate the ground from the probes exposed to plasma. This isolation was found to be extremely necessary in order to prevent any stray discharge taking place between the grounded electrodes and the main electrodes.

The velocity u, calculated from the experiment was found to be less than the value found by previous methods indicating that the flow velocity is smaller than the velocity exhibited by the luminous front.

The application of an axial magnetic field did not produce any detectable effect more than the range of the experimental error. Values up to 950 Gauss of magnetic field were applied. Typical oscilloscope traces for cases with and without magnetic field are shown in Fig. 28. The time delay produced, if any, may be due to the fringing of the magnetic field lines. No temperature measurements were made in this part of the experiment.

The Effect of a Transverse Magnetic Field on the Axial Electric Field

The axial electric field was studied using the differential E_z probes discussed earlier. Specifically, the probes were used to monitor the effect a transverse magnetic field would have on the axial electric field.

Electrons at the wave front, due to their large mobility lead the ion population. The charge separation produced results in an axial electric field. As the ionized gas flows through a magnetic field, electrons would start to gyrate with a much smaller radius around the

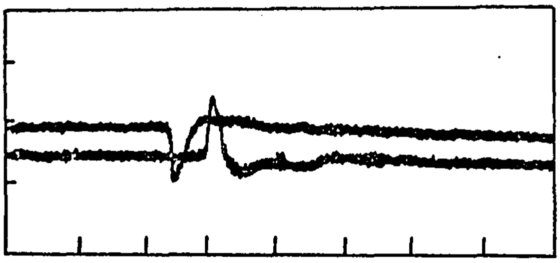

1 μsec/cm
1 v/cm

Figure 27. Oscillogram of the probe voltage with the magnetic induction for +B and -B.

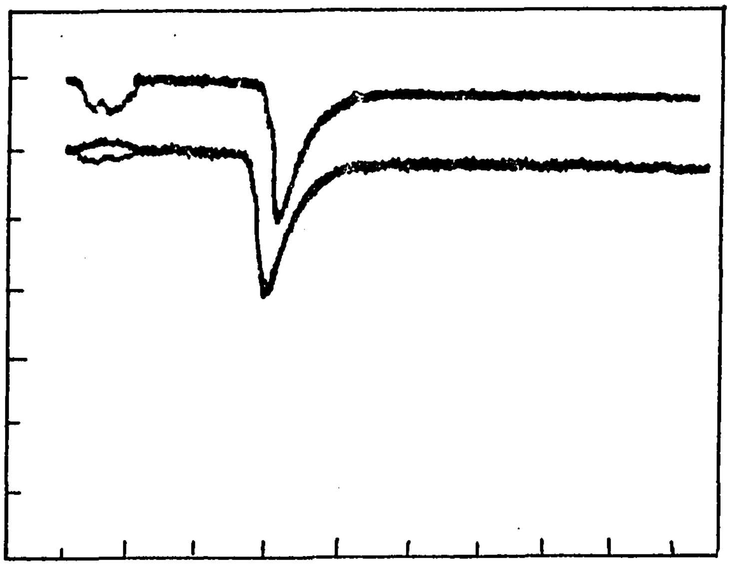

Effect due to axial B-field

Top, B = 0

Bottom, B = 900 Gauss

Figure 28. Oscillogram of probe voltage with and without axial magnetic field.

magnetic field lines than the ions. The retardation on electrons in the axial direction would be much larger than on the ions. This was demonstrated by the delay time produced by the transverse magnetic field. This difference in the axial velocity of the charged species should decrease the axial electric field intensity.

For a critical value of the B-field one expects the electric field force on the electrons to become equal to the magnetic force, i.e.

$$evB = eE_z \ .$$

This critical value of B-field was measured to be about 1600 Gauss. If the measured values, $v = 8\times10^5$ m/sec, and $B = 0.1$ web/m^2 are substituted into the above relation, then in order for the relation to hold E_z must be equal to 1.28×10^5 v/m, which agrees with the direct measured value of E_z within a factor 3.

A number of E_z oscilloscope traces for different values of magnetic field intensity are shown in Fig. 29. Note how the critical value of B is approached as the value of B is increased. The delay time brought about by the field is also easily observable from the figures.

The Electric Field

The final parameter of interest is the electric field operating in the precursor. The results previously obtained by the introduction of the axial field probes inside the shock tube were able to give only the value of the maximum space charge operating at the wave front. It would be of particular interest to know how the field is changing through the wave along the axis of the shock tube. This information was obtained as follows.

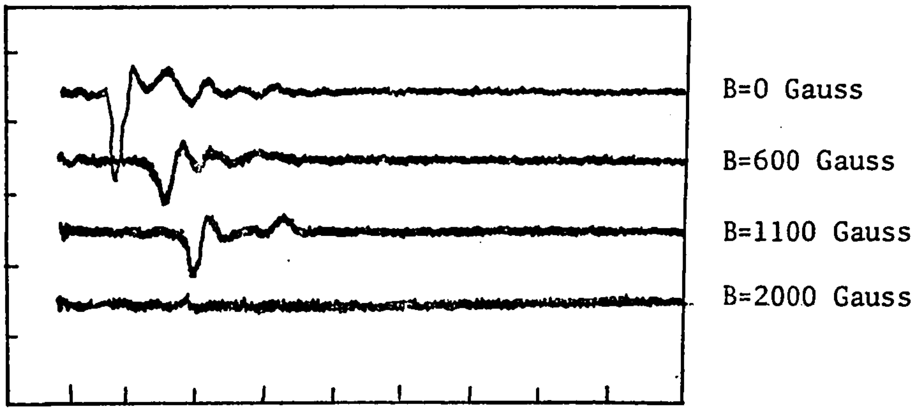

Figure 29. Oscillograms of the axial electric field for different values of magnetic full intensity.

One of the differential electric field probes discussed earlier was placed directly outside the tube walls and in three different orientations in order to monitor E_z, E_r, and E_θ. These probes are essentially dipole antennas and are capable of monitoring the time varying electric field.

The probes were used outside of the shock tube and thus in a position where they could not effect the flow of the wave or disturb the electric field configuration around the wave. It has been mentioned that these probes were coaxially constructed in such a way as to elluminate inductive loops which might give rise to spurious signals. The probes were calibrated so that the signals as monitored on an oscilloscope, could be translated into volts/cm in the plasma. Corrections for the probes response at different frequencies were made.

The probes were positioned 30 cm down the sidearm and the signals were compared to the output of a PM tube located at the same position. The signals for E_r and E_θ were approximately $\frac{1}{4}$ the value of the signals for E_z. A typical oscillogram of E_z, compared to PM output, is shown in Fig. 30. The field appears some 200 nsec before the luminosity of the front. In other words the field must be present before the electrical breakdown of the gas occurs. The maximum amplitude of the probe signals corresponds to about 400 v/an. This value will depend, of course, on the experimental parameters such as applied voltage, pressure, etc.

The time dependence of the probe output demonstrates two things. It tells us first of all that the electric field associated with the wave is a maximum in advance of the wave, decreases in the region of the wave front, and finally approaches zero in the ionized gas behind

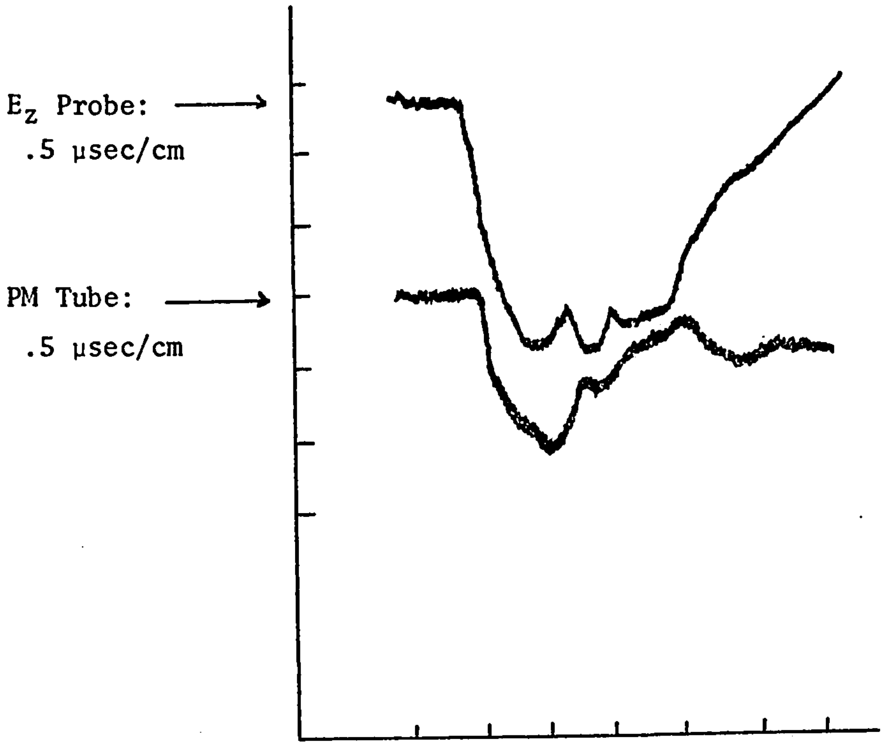

Differential probe measurement of axial electric field compared to optical onset 30 cm down side arm.

Figure 30. Oscillogram of Electromagnetic field vs PM oscillogram.

the wave. Secondly, we see that the precursor is caused chiefly by the quasi-DC base frequency of the capacitor. There are apparently no higher frequencies present, thus indicating that the wave has no dependence on any RF which may be generated during driver discharge.

CHAPTER IV

CONCLUSIONS AND COMMENTS

This work has been successful in isolating the component causes of precursive effects in the electrical shock tube. Although some light scattering accompanied by photoionization as well as an electron diffusion phenomenon is present, it has become clear that the main component of the electrical shock tube precursor is an induction driven breakdown wave augmented by heat conduction. The wave is not driven by the voltage applied to the capacitor, as is generally true of breakdown waves, but rather by the voltage induced by the interaction of the current time rate of change with the mutual inductance of the system.

This kind of induction driver breakdown wave will always be present to some degree in any electrical shock tube unless proper grounding procedures are followed. It is now clear why some observers have failed to see a fluid dynamical precursor operating in their apparatus.

The experimental parameters of the precursor breakdown wave have been thoroughly analyzed and agree, at least qualitatively, with the behavior of the common kind of breakdown wave investigated, for example, by Blais and Haberstitch. The results suggest, however, that neither the results of Blais and Haberstitch nor the theoretical analysis of breakdown waves by Shelton is directly applicable to the electrical shock tube precursor. This discrepancy is a result of the additional transfer of energy to the front due to heat conduction in the shock tube precursor.

Several suggestions can be made which justify the need for further research. Blais observed that his waves appeared to propagate with constant velocity after reaching a certain distance and the hint of such behavior was noticed in this work. The velocity involved was found to be lower than the limit predicted by Shelton in his analysis of breakdown waves. Increasing the distance between the ground electrode in the shock tube would allow one to study the behavior of the wave at greater distances from the driver and more complete investigations of the precursor's attenuation would then be possible.

It would also be interesting to study the precursor over a larger assortment of discharge circuit geometries. One would then be able to predict the magnitude of precursive effects between the extremes of no induced voltage and an induced voltage approaching the applied capacitor voltage. A greater range of pressure would be desirable too.

Finally it would be instructive to look at precursors driven by self inductance instead of mutual inductance. This technique of generating driving voltage should be just as effective and is probably the primary cause of precursors in shock tubes employing a T-tube geometry.

In short, the nature of the electrical shock tube precursor is now clear and furthermore it becomes apparent that any one who uses the electrical shock tube as a research tool now has the capability to create or eliminate precursors of this type at will.

BIBLIOGRAPHY

1. F. Hauksbee, Philosophical Transactions of the Royal Society *XXV* (Issue 307), 2277-2282 (1706).

2. C. Wheatstone, Pogg. Ann. *34*, 148 (1835).

3. W. Von Zahn, Pogg. Ann. 675 (1879).

4. J. J. Thomson, Recent Researches (Oxford University Press, New York, 1893), p. 115.

5. J. W. Beams, Phys. Rev. *36*, 997 (1930).

6. L. B. Snoddy, J. W. Beams, and J. R. Dietrich, Phys. Rev. *52*, 739 (1937).

7. F. H. Mitchell and L. B. Snoddy, Phys. Rev. *72*, 1202 (1947).

8. L. B. Snoddy, J. W. Beams and J. R. Dietrich, Phys. Rev. *50*, 469 (1936).

9. A. V. Nedospasov and A. E. Novik, Soviet Phys. - Tech. Phys., *5*, 1261 (1961).

10. R. N. Hollyer, Jr., Johns Hopkins University, Applied Physics Laboratory, Rept. No. CM-903 (May 1957).

11. V. Josephson and R. W. Hales, Space Tech. Lab Report STL/TR-60-0000-19313; Phys. Fluids *4*, 373 (1961).

12. H. D. Weymann, The Physics of Fluids *3*, 545-548 (1960).

13. E. A. McLean, A. C. Kolb and H. R. Griem, Physics of Fluids *4*, 1055 (1961).

14. R. G. Fowler and J. D. Hood, The Physical Review *128*, 991-2 (1962).

15. G. W. Paxton and R. G. Fowler, Phys. Rev. *128*, 993 (1962).

16. G. A. Shelton, Ph.D. Dissertation, University of Oklahoma (1967).

17. Lubin and Resler, Phys. Fluids *10*, 1 (1957).

18. M. J. Lubin, Phys. Fluids *10*, 1794 (1967).

19. L. B. Snoddy, J. W. Beams, and J. R. Dietrich, Phys. Rev. *50*, 469 (1936).

20. A. Haberstitch, "Experimental and Theoretical Study of an Ionizing Potential Wave in a Discharge Tube," Ph.D. Dissertation, University of Maryland (1964).

21. G. Russell, Phys. of Fluids *12*, 1216 (1969).

22. P. Liou, "Precursor Wave Speed Measurements in Electron-Driven Linear Shock Tube," M.S. Thesis, University of Oklahoma (1971).

23. I. D. Latimer, J. I. Mills, and R. A. Day, Journal of Quantitative Spectroscopy and Radiative Transfer *10*, 629 (1970).

24. J. P. Appleton, Phys. Fluids *9*, 336 (1966).

25. R. G. Fowler, "Electrically Energized Shock Tubes" (Research Institute), University of Oklahoma, Norman, Oklahoma (1963).

26. R. N. Blais, "The Electrical Breakdown of Helium," Ph.D. Dissertation, University of Oklahoma (1971).

27. R. Isler, and D. Kerr, Phys. Fluids *8*, #6 (1965).

28. R. M. St. John, Methods of Exp. Physics *8*, (1969).

29. F. L. Miller, Ph.D. Dissertation, University of Oklahoma (1964).

30. I. D. Latimer, unpublished.

APPENDIX

THE COMPUTER ANALYSIS FOR ELECTRON TEMPERATURE MEASUREMENTS

It has been mentioned earlier that the electron temperature analysis involved the expression

$$\frac{1/A_{jk}f_{jk}\ dI_{jk}/dt + I_{jk}/f_{jk}}{1/A_{\ell m}f_{\ell m}\ dI_{\ell m}/dt + I_{\ell m}/f_{\ell m}} = \frac{(\sigma_{jk}v)}{(\sigma_{\ell m}v)} \ .$$

Experimentally one proceeds as follows. The oscillograms for the two spectral lines were enlarged with an opaque projector onto graph paper and the values for I_{jk} and I_{ma} were read off at ten nanosecond intervals and converted into inches. Sample graphs for the He 5048 line and He 4713 line are shown in Figs. 31 and 32.

These values of intensity were fed into a computer program which computed the left hand ratio of the expression (1) above. The calculated ratio of intensity as a function of time was then compared to the tabulated results of Latimer, Mills and Day for the right hand ratio of expression (1). The electron temperature as a function of time was then known.

The analysis of the time varying case was done by Dr. R. G. Fowler, and Mr. Robert Jayroe developed the computer program which calculates the intensity ratios. The program was originally intended for use on the GE 430 time share computer system and was later modified by Mr. C. T. Bush and the author for use on the IBM 1130 computer at the

APPENDIX

THE COMPUTER ANALYSIS FOR ELECTRON TEMPERATURE MEASUREMENTS

It has been mentioned earlier that the electron temperature analysis involved the expression

$$\frac{dI_{jk}/dt+A_{jk}I_{jk}}{dI_{\ell m}/dt+A_{\ell m}I_{\ell m}} = \frac{(\sigma_j v)}{(\sigma_\ell v)}$$

Experimentally one proceeds as follows. The oscillograms for the two spectral lines were enlarged with an opaque projector onto graph paper and the values for I_{jk} and I_{ma} were read off at ten nano-second intervals and converted into inches. Sample graphs for the He 5048 line and He 4713 line are shown in Figs. 31 and 32.

These values of intensity were fed into a computer program which computed the left hand ratio of the expression (1) above. The calculated ratio of intensity as a function of time was then compared to the tabulated results of Latimer, Mills and Day for the right hand ratio of expression (1). The electron temperature as a function of time was then known.

The analysis of the time varying case was done by Dr. R. G. Fowler, and Mr. Robert Jayroe developed the computer program which calculates the intensity ratios. The program was originally intended for use on the GE 430 time share computer system and was later modified by Mr. C. T. Bush and the author for use on the IBM 1130 computer at the

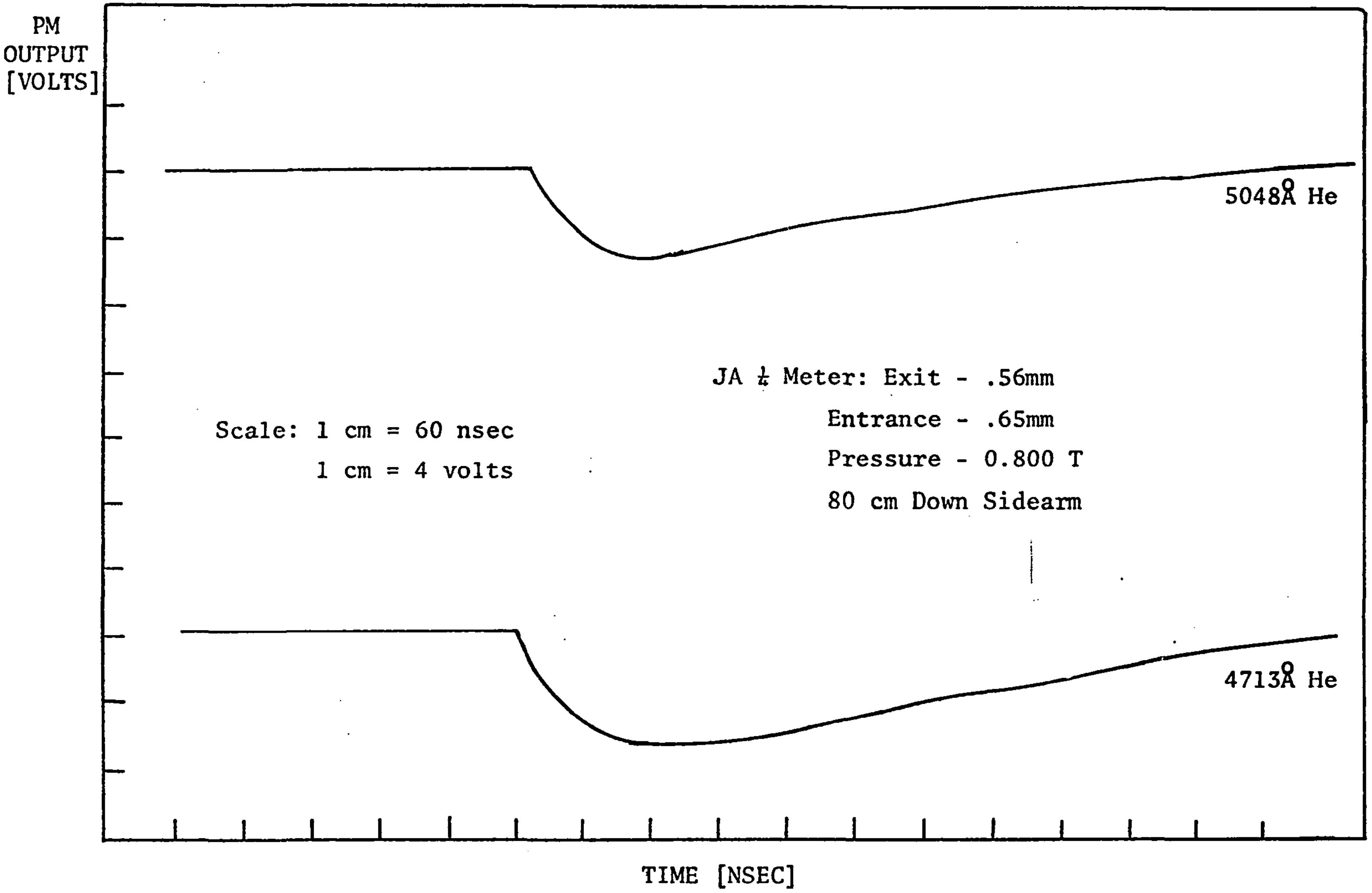

Figure 31. Graph of 5048 He

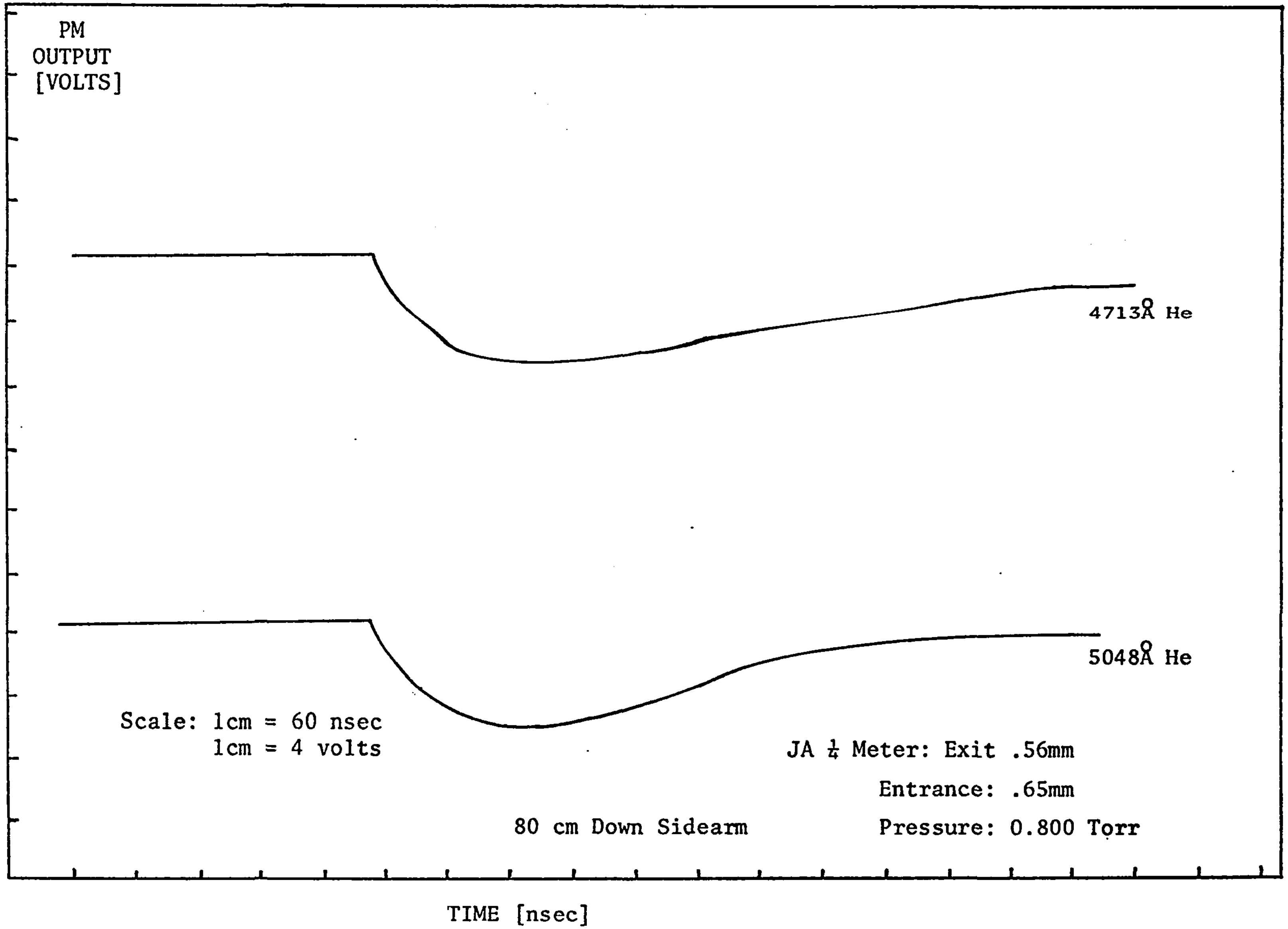

Figure 32. Graph of 4713 He.

University of Oklahoma. The program listing and an example output are presented on the following pages.

```
READY
ZDIT PAGE
--------

KTY2      FRI.      08/14/70
  #01

100$NDM
110            DIMENSION DEL(40,40),Y(40),Z(40),U(40),V(40)
120            PRINT,"ENTIRE NUMBER OF DATA POINTS"
130            INPUT,NDAT
140            PRINT,"ENTER FINITE DIFFERENCE ORDER"
150            INPUT,NTH
160            PRINT,"ENTER ABSCISSA INCREMENT"
170            INPUT,DW
180            PRINT,"ENTER ORDINATE SCALE FACTOR"
190            INPUT,SCL
200            MAX=NDAT-1
210            KOUNT=0
220        10  PRINT,"ENTER ORDINATE VALUES"
230            INPUT,(Y),1=1,NDAT)
240            PRINT,"ENTER LIFETIME"
250            INPUT,A
260            DO 20 1=1,NDAT
270            Z(1)=Y(1)
280        20  CONTINUE
290            DO 50 1=1,MAX
300            K=1+1
310            DO 30 J=K,NDAT
320            KX=J-1
330            DEL(I,J)=Y(J)-Y(KX)
340        30  CONTINUE
350            DO 40 J=K,NDAT
360            Y(J)=DEL(I,J)
370        40  CONTINUE
380        50  CONTINUE
390            DO 70 J=1,MAX
400            SUM=0.0
410            K-MAX-J+1
420            IF(K-NTH)58,58,57
430        57  K=NTH
440        58  DO 60 1=1,K
450            L=I+J
460            IF(1-2*(I/2))54,55,54
470        54  SUM=SUM+DEL(I,L)/I
480            GO TO 60
490        55  SUM=SUM-DEL(I,L)/I
500        60  CONTINUE
510            Y(J)=SUM/DW
520        70  CONTINUE
```

```
      IF(KOUNT)140,80,140
 80   DO 90 I=1, MAX
      U(I)=Y(I)*SCL
      V(I)=(Z(I)/A+Y(I)*SCL
 90   CONTINUE
      T=0.0
      PRINT"LIST F1',G1=A1*F1+f1'?-NO=0;YES=1"
      INPUT,ILST
      IF(ILST)100,120,100
100   DO 110 I=1,MAX
      PRINT,U(I),V(I),T
      T=T+DW
110   CONTINUE
120   PRINT,"CALCULATE F8',G2=A2*F2+D2'?-NO=0;YES=1"
      INPUT,ICAL
```

```
KTY2      FRI.   08/14/70
  #02

      IF(ICAL)130,200,130
130   KOUNT=1
      GO TO 10
140   DO 150 I=1,MAX
      Z(I)=(Z(I)/A+Y(I)*SCL
150   CONTINUE
      T-0.0
      PRINT,"LIST F2',G2=A2*F2'?-NO=0'YES=1"
      INPUT,ILST
      IF(ILST)160,180,160
160   DO 170 I=1,MAX
      Y(I)=Y(I)*SCL
      PRINT,Y(I),Z(I),T
      T=T+DW
170   CONTINUE
      T=0.0
180   PRINT,"G1
      DO 190 I=1,MAX
      U(I)=V(I)/Z(I)
      PRINT,V(I),Z(I),U(I),T
      T=T+DW
190   CONTINUE
200   CONTINUE
      END
```

```
PYSOPWHARING SERVICE

ON AT- 13:34  PORT:31

USER #? S380

PASSWORD

MMXXM?

OLD/NEW? OLD:KTY2

READY
RUNNH
.
ENTER NUMBER OF DATA POINTS
? 30

ENTER FINITE DIFFERENCE ORDER
? 1

ENTER ABSCISSA INCREMENT
? 14.8

ENTER ORDINATE SCALE FACTOR
? 8.5

ENTER ORDINATE VALUES
? .16,.22,.31,.34,.47,.44,.5,.47,.47,.47,.44,.41,.38,.38,.34,
? .31,.31,.28,.28,.25,.25,.22,.22,.22,.19,.19,.19,.16,.13,.13

ENTER LIFETIME
? 89

LIST F1',G1=A1*F1+F1'?-NO=0;YES=1
? 1

   3.445945946E-02     4.974035833E-02     0.000000000E+00
   5.168918919E-02     7.270042514E-02     1.480000000E+01
   1.722972973E-02     4.683647130E-02     2.960000000E+01
   7.466216216E-02     1.071340722E-01     4.440000000E+01
  -1.722972973E-02     2.765771072E-02     5.920000000E+01
   3.445945946E-02     7.648193137E-02     7.400000000E+01
  -1.722972973E-02     3.052307926E-02     8.880000000E+01
   0.000000000E+00     4.488764045E-02     1.036000000E+02
   0.000000000E+00     4.488764045E-02     1.184000000E+02
  -1.722972973E-02     2.765791078E-02     1.332000000E+02
  -1.722972973E-02     2.479274218E-02     1.480000000E+02
  -1.722972973E-02     2.192757364E-02     1.628000000E+02
   0.000000000E+00     3.629213483E-02     1.776000000E+02
  -2.297297297E-02     1.331916156E-02     1.924000000E+02
  -1.722972973E-02     [illegible].524215038E-02     2.072000000E+02
   0.000000000E+00     2.960674157E-02     2.220000000E+02
  -1.722972973E-02     1.237701184E-02     2.368000000E+02
   0.000000000E+00     2.674157303E-02     2.516000000E+02
  -1.722972973E-02     9.511843304E-03     2.664000000E+02
   0.000000000E+00     2.387640449E-02     2.812000000E+02
  -1.722972973E-02     6.646674744E-03     2.960000000E+02
   0.000000000E+00     2.101123595E-02     3.108000000E+02
```

```
 -1.722972973E-02   9.511843304E-03   2.664000000E+02
  0.000000000E+00   2.387640449E-02   2.812000000E+02
 -1.722972973E-02   6.646674764E-03   2.960000000E+02
  0.000000000E+00   2.101123595E-02   3.108000000E+02
  0.000000000E+00   2.101123595E-02   3.256000000E+02
 -1.722972973E-02   3.781506225E-03   3.404000000E+02
  0.000000000E+00   1.814606742E-02   3.552000000E+02
  0.000000000E+00   1.814606742E-02   3.700000000E+02
 -1.722972973E-02   9.163376862E-04   3.848000000E+02
 -1.722972973E-02  -1.948830854E-03   3.996000000E+02
  0.000000000E+00   1.241573033E-02   4.144000000E+02
CALCULATE F2',G2=A2*F2+F2'?-NO=0;YES=1
? 1

ENTER ORDINATE VALUES
? .19,.25,.37,.44,.5,.53,.56,.56,.56,.56,.56,.56,.53,.53,.5,
? .5,.5,.5,.5,.5,.5,.5,.5,.5,.47,.47,.44,.4,.38,.38,.37

ENTER LIFETIME
? 62

LIST F2',G2=A2*F2+F2'?-NO=0;YES=1
? 1

  3.445945946E-02   6.050784656E-02   0.000000000E+00
  6.891891892E-02   1.031931124E-01   1.480000000E+01
  4.020270270E-02   9.092850915E-02   2.960000000E+01
  3.445945946E-02   9.478204010E-02   4.440000000E+01
  1.722972973E-02   8.577811683E-02   5.920000000E+01
  1.722972973E-02   8.959102005E-02   7.400000000E+01
  0.000000000E+00   7.677419355E-02   8.880000000E+01
  0.000000000E+00   7.677419355E-02   1.036000000E+02
  0.000000000E+00   7.677419355E-02   1.184000000E+02
  0.000000000E+00   7.677419355E-02   1.332000000E+02
  0.000000000E+00   7.677419355E-02   1.480000000E+02
 -1.722972973E-02   5.954446382E-02   1.628000000E+02
  0.000000000E+00   7.266129032E-02   1.776000000E+02
 -1.722972973E-02   5.543156059E-02   1.924000000E+02
  0.000000000E+00   6.854838710E-02   2.072000000E+02
  0.000000000E+00   6.854838710E-02   2.220000000E+02
  0.000000000E+00   6.854838710E-02   2.368000000E+02
  0.000000000E+00   6.854838710E-02   2.516000000E+02
  0.000000000E+00   6.854838710E-02   2.664000000E+02
  0.000000000E+00   6.854838710E-02   2.812000000E+02
  0.000000000E+00   6.854838710E-02   2.960000000E+02
  0.000000000E+00   6.854838710E-02   3.108000000E+02
  0.000000000E+00   6.854838710E-02   3.256000000E+02
 -1.722972973E-02   5.131865737E-02   3.404000000E+02
  0.000000000E+00   6.443548387E-02   3.552000000E+02
 -1.722972973E-02   4.720575414E-02   3.700000000E+02
 -2.297297297E-02   3.734960767E-02   3.848000000E+02
 -1.148648648E-02   4.335222319E-02   3.996000000E+02
  0.000000000E+00   5.209677419E-02   4.144000000E+02
G1                  G2                G1/G2
  4.974035833E-02   6.050784656E-02   8.220480676E-01   0.000000000E+[illegible]

  7.270042514E-02   1.031931124E-01   7.045085026E-01   1.480000000E+[illegible]

  4.683647130E-02   9.092850915E-02   5.150911605E-01   2.960000000E+[illegible]

  1.071340722E-01   9.478204010E-02   1.130320387E+00   4.440000000E+[illegible]

  [illegible]
```

3.052307926E-02	7.677419355E-02	3.975695198E-01	8.880000000E+01
4.488764045E-02	7.677419355E-02	5.846709470E-01	1.036000000E+02
4.488764045E-02	7.677419355E-02	5.846709470E-01	1.184000000E+02
2.765791072E-02	7.677419355E-02	3.602500976E-01	1.332000000E+02
2.479274218E-02	7.677419355E-02	3.229306755E-01	1.480000000E+02
2.192757364E-02	5.954446382E-02	3.682554554E-01	1.628000000E+02
3.629213483E-02	7.266129032E-02	4.994700021E-01	1.776000000E+02
1.331916186E-02	5.543156059E-02	2.402811993E-01	1.924000000E+02
1.524218038E-02	6.854838710E-02	2.223565138E-01	2.072000000E+02
2.960674157E-02	6.854838710E-02	4.319101124E-01	2.220000000E+02
1.237701184E-02	6.854838710E-02	1.805587610E-01	2.368000000E+02
2.674157303E-02	6.854838710E-02	3.901123595E-01	2.516000000E+02
9.511843304E-03	6.854838710E-02	1.387610082E-01	2.664000000E+02
2.387640449E-02	6.854838710E-02	3.483146067E-01	2.812000000E+02
6.646674764E-03	6.854838710E-02	9.696325538E-02	2.960000000E+02
2.101123595E-02	6.854838710E-02	3.065168539E-01	3.108000000E+02
2.101123595E-02	6.854838710E-02	3.065168539E-01	3.256000000E+02
3.781506225E-03	5.131865737E-02	7.368677240E-02	3.404000000E+02
1.814606742E-02	6.443548387E-02	2.816160650E-01	3.552000000E+02
1.814606742E-02	4.720575414E-02	3.844037183E-01	3.700000000E+02
9.163376862E-04	3.734960767E-02	2.453406457E-02	3.848000000E+02
-1.948530854E-03	4.335222319E-02	-4.495342361E-02	3.996000000E+02
1.241573033E-02	5.209677419E-02	2.383205204E-01	4.144000000E+02

RAN: 05.7 SECS

READY
BYE

OFF AT